Biosystems, Foster City, CA, USA) was used for PCR amplification. The amplification program used was 35 cycles of 30 s at 94°C, 30 s at 64°C, and 40 s at 72°C, with a final incubation of 7 min at 72°C.

Flow cytometry and cell sorting

Cultured cells were incubated with enzyme-free Hank's-based Cell Dissociation Buffer (Invitrogen) for 30 min at 37°C and gently dissociated into single cells. The cells were then washed with PBS twice, probed with biotinylated-SM/C-2.6 (23) antibody for 15 min at room temperature, and stained with phycoerythrin-conjugated strepavidin (12-4312; eBioscience, San Diego, CA, USA) for 15 min at room temperature. Dead cells were excluded from the plots based on propidium iodide staining (Sigma), and SM/C-2.6-positive cells were collected using a FACS Vantage instrument (Becton Dickinson, San Jose, CA, USA). Sorted cells were plated (1×10^4 cells/well) with differentiation medium in 96-well plates (Falcon) coated with Matrigel (008504; BD Bioscience). The medium was changed every 5 d, and 7 d after plating the cultured cells were analyzed.

Intramuscular cell transplantation (primary transplantation)

Recipient mice were injected with 50 μl of 10 μM cardiotoxin (CTX; Latoxan, Valence, France) (30) in the LTA muscle 24 h before transplantation (31). CTX is a myotoxin that destroys myofibers, but not satellite cells, and leaves the basal lamina and microcirculation intact. Since proliferation of host myogenic cells may prevent the incorporation of transplanted cells, recipient mdx mice (15) received 8 cGy of systemic irradiation (32) 12 h before transplantation to block muscle repair by endogenous cells. An average of 4.53×10^4 ES-derived SM/C-2.6-positive or -negative cells were washed twice with 500 μl of PBS, resuspended in 20 μl of DMEM, and injected into the LTA muscle of recipient mdx mice using an allergy syringe (Becton Dickinson). Mdx mice, which are derived from the CL/B16 strain, were used as the recipient mice in all experiments. Similarly, D3 ES cells, which are derived from the 129X1/SvJ ES cells, were used in all experiments. The major histocompatibility complex (MHC) of mdx mouse and D3 cells are very similar, both possessing type *b* MHC H2 haplotypes. All animal-handling procedures followed the Guild for the Care and Use of Laboratory Animals published by the U.S. National Institutes of Health (NIH Publication No. 85-23, revised 1996) and the Guidelines of the Animal Research Committee of the Graduate School of Medicine, Kyoto University.

Secondary transplantation

The LTA muscles of recipient mice were collected 8 wk after the primary transplantation. The muscles were minced and digested into single cells with 0.5% collagenase type I (lot S4D7301; Worthington Biochemical Corp., Lakewood, NJ, USA). After washing with PBS and filtration through a 100 μm filter, Pax7-positive cells were sorted by FACS using the SM/C-2.6 antibody. SM/C-2.6-positive cells (200 cells/mouse) were injected into preinjured LTA muscles of secondary recipient mice. The LTA muscles were analyzed 8 wk after transplantation.

Isolation and immunostaining of single fibers

To detect muscle satellite cells attaching to single fibers with Pax7, muscle fibers from the LTA muscle of recipient mice were prepared essentially according to the method of Bischoff in Rosenblatt *et al.* (33). Briefly, dissected muscles were incubated in DMEM containing 0.5% type I collagenase (Worthington) at 37°C for 90 min. The tissue was then transferred to prewarmed DMEM containing 10% FBS. The tissue was gently dissociated into single fibers by trituration with a fire-polished wide-mouth Pasteur pipette. Fibers were transferred to a Matrigel-coated 60 mm culture dish (Falcon) and fixed in 4% PFA for 5 min at room temperature. Fibers were permeabilized with 0.1% Triton X-100 in PBS for 10 min, and nonspecific binding was blocked by incubation in 5% skim milk for 10 min at room temperature. Primary mouse monoclonal antibodies against mouse Pax7 were applied for 12 h at 4°C. Antibodies were detected using the secondary antibodies described above.

Statistics

Data are presented as means ± SD. For comparison of the numbers of MHC and Pax7-positive cells in the sorted SM/C-2.6-positive and -negative fractions and the numbers of GFP-positive muscle fascicles and GFP/Pax7-double-positive cells in reinjured and noninjured groups, the unpaired Student's t test was used, and a value of $P < 0.05$ was considered to be statistically significant.

RESULTS

Myogenic lineage cells are effectively induced from mES cells *in vitro*

EBs were formed in hanging drop cultures for 3 d followed by an additional 3 d in suspension cultures (**Fig. 1*A***). These EBs were then plated onto Matrigel-coated 48-well plates in differentiation medium, which contained 5% HS. This culture method is a modified version of the classical ES cell differentiation method (25) and the skeletal muscle single fiber culture method (33). After plating, EBs quickly attached to the bottom of the coated dishes, and spindle-shaped fibers appeared surrounding the EBs by the seventh day of plating (d 3+3+7; Fig. 1*B*). As these spindle fibers grew, they began to fuse with each other, forming thick multinucleated fibers resembling skeletal myofibers (Fig. 1*C, D*). At the same time we observed spontaneous contractions by the fibers (Supplemental Videos 1 and 2), a trait commonly seen in cultured skeletal muscle fibers. Immunostaining showed that these fused fibers were positive for skeletal-muscle-specific MHC (Fig. 1*E*). Furthermore, cells expressing muscle regulatory factor (MRF) proteins, including Pax7 (Fig. 1*F*), Myf5 (Fig. 1*G*), MyoD (Fig. 1*H*), and myogenin (Fig. 1*I*) were observed. On d 3 + 3 + 14, the average number of MHC-positive wells was 73.6 ± 5.8% (n=144). In all the MHC-positive wells, cells expressing Pax7, an essential transcription factor in satellite cells, were also observed. Double staining for Pax7 and MyoD confirmed the existence of cells staining for Pax7 alone, indicating the presence of quiescent-state satellite cells (34) within the culture (Supplemental Fig. 1). Next, the time course of MRF expression was examined by RT-PCR (Fig. 1*J*). Expression of Pax3 and Pax7 both peaked on d 3 + 3 +

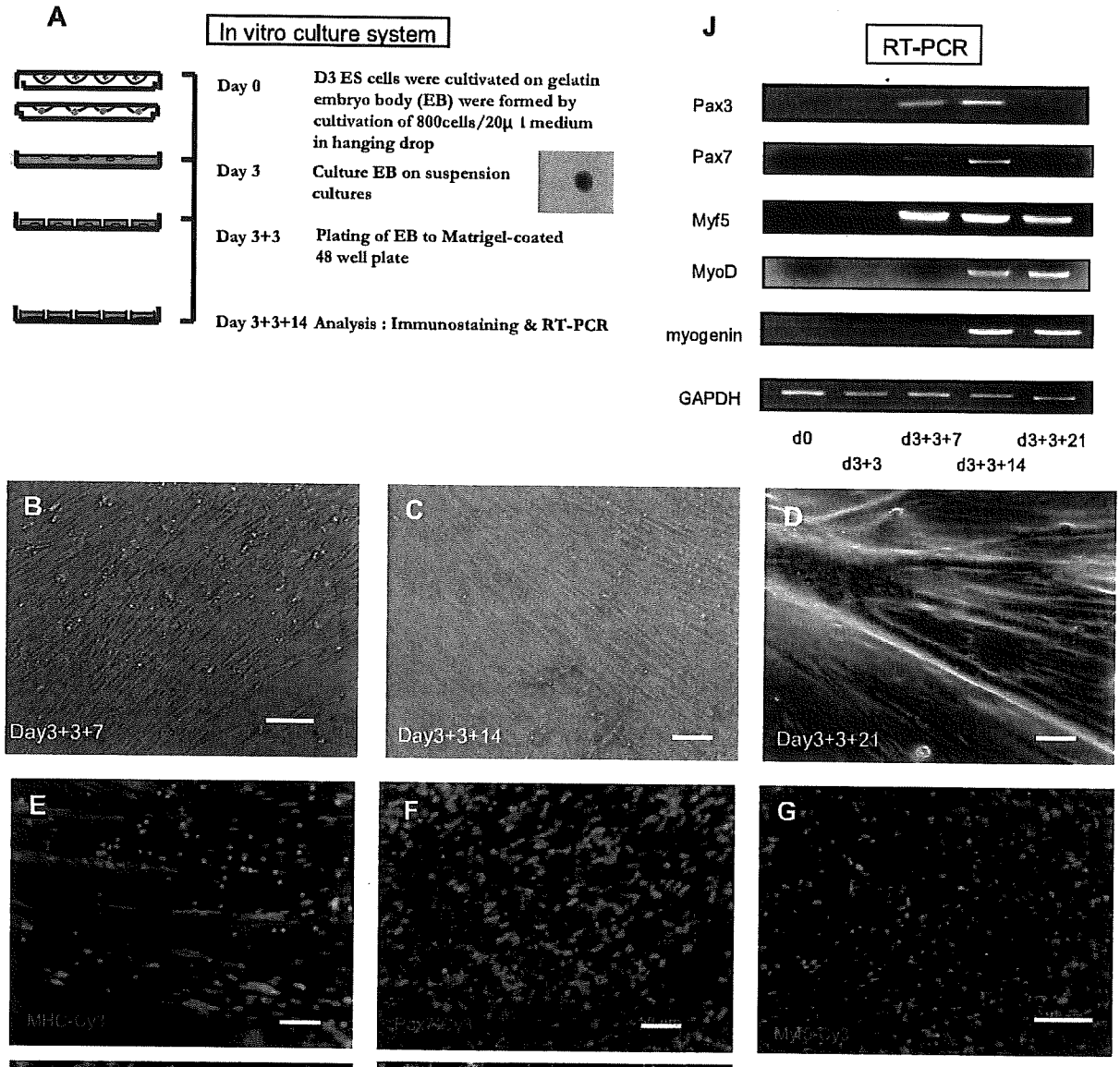

Figure 1. Effective induction of myogenic lineage cells from mES cells *in vitro*. *A*) *In vitro* culture system for ES cells. *B–E*) Skeletal myofibers observed within the culture system (*B–D*), which were positive for the mature myofiber marker MHC (*E*). *F, G*) Commonly recognized markers for satellite cells, Pax7 (*F*) and Myf5 (*G*), were observed in the cultures. *H, I*) MyoD-positive (*H*) and myogenin-positive fibers (*I*) were also observed in the cultures. White boxes indicate multinucleated myotubes (*I*). *J*) RT-PCR expression of MRFs including Pax3, Pax7, Myf5, MyoD, and myogenin in ES cells in our novel culture system at d 0, 3 + 3, 3 + 3 + 7, 3 + 3 + 14, and 3 + 3 + 21. Scale bars = 50 μm (*A–F*); 100 μm (*G–I*).

14, but Myf5, MyoD, and myogenin continued to be expressed after d 3 + 3 + 14.

Thus, using Matrigel plates and differentiation medium containing HS, myogenic lineages including Pax7-positive satellite-like cells were successfully induced from mES cells.

A novel antibody, SM/C-2.6, can enrich for Pax7-positive satellite-like cells derived from ES cells

To examine the characteristics of ES-derived Pax7-positive satellite-like cells, we needed to isolate these cells from the culture. Since Pax7 is a nuclear protein rather than a

surface marker, anti-Pax7 antibodies cannot be used for living cell separation by FACS. Therefore, a novel antibody, SM/C-2.6 (23), was used to detect satellite cells. SM/C-2.6 detects quiescent adult mouse satellite cells, as well as satellite cells in neonatal muscle tissue, as determined by immunostaining (Supplemental Fig. 2). RT-PCR confirmed that sorted SM/C-2.6-positive cells expressed Pax3, Pax7, Myf5, and c-met, whereas sorted SM/C-2.6-negative cells did not (Supplemental Fig. 3). Thus, the SM/C-2.6 antibody was shown to be useful for isolating living satellite cells by FACS.

We collected all the differentiated ES cells (1×10^6 cells) from cultures on d 3 + 3 + 14. FACS analysis using the SM/C-2.6 antibody showed that 15.7% of the cells were SM/C-2.6 positive (**Fig. 2A**). RT-PCR analysis revealed that sorted SM/C-2.6-positive cells strongly expressed Pax3, Pax7, Myf5, c-met, and M-cadherin (Fig. 2*B*). Using a cytospin preparation of sorted SM/C-2.6-positive cells, we also confirmed the expression of M-cadherin (Fig. 2*C*) and Pax7 (Fig. 2*D*; 70.7±16.5% and 59.9±1.1% positive, respectively); only 2.3 ± 0.49% of the sorted SM/C-2.6-negative cells expressed M-cadherin, and 2.7 ± 0.1% expressed Pax7. Thus, the SM/C-2.6 antibody could enrich for satellite-like cells derived from mES cells *in vitro*.

ES-derived satellite-like cells have strong myogenic potential *in vitro*

To evaluate the myogenic potential of ES-derived SM/C-2.6-positive satellite-like cells *in vitro*, both SM/C-2.6-positive and -negative cells were sorted by FACS and plated in 96-well Matrigel-coated plates (see Fig. 4A). One week after cultivation, the number of muscle fibers in the wells was assessed. Although there were fibroblast-like and endothelium-like cells, MHC-positive fibers (787.3±123.7/well, 10.7±0.8% of the total cells per well, n=3) and Pax7-positive cells (222±81.4/well, 2.9±1.1% of the total cells per well, n=9) were observed in the SM/C-2.6-positive wells. In contrast, very few MHC-positive fibers (8.75±32.6/well, n=15; 0.12±0.46%) or Pax7-positive cells (2.6±2.0/well, n=8; 0.03±0.01%) were seen in the SM/C-2.6-negative wells

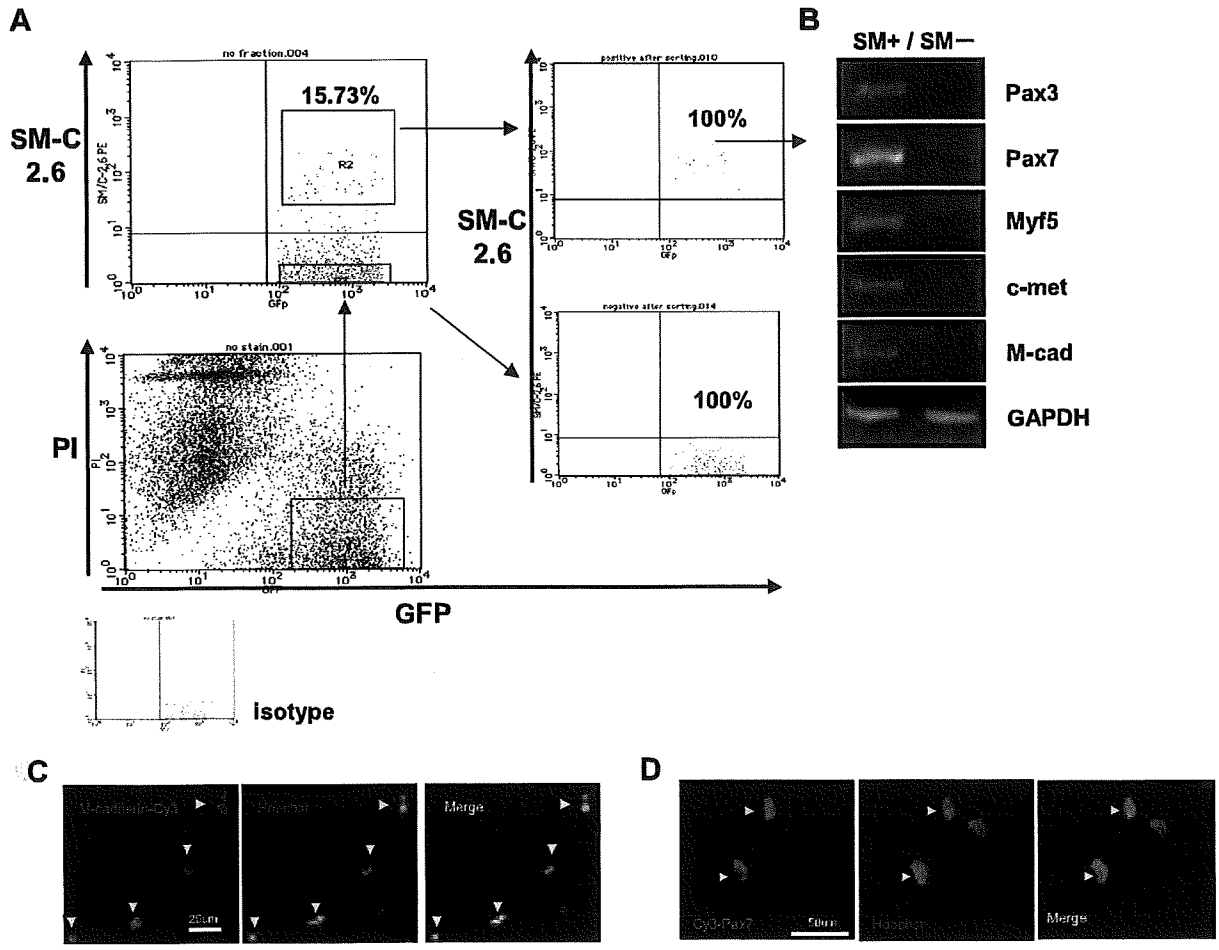

Figure 2. A novel antibody, SM/C-2.6, can enrich Pax7-positive satellite-like cells derived from ES cells. *A*) FACS data of cultured ES cells at d 3 + 3 + 14 indicate that 15.7% of total cultured cells are SM/C-2.6-positive cells. *B*) RT-PCR of the SM/C-2.6-positive fraction showed strong expression of Pax3, Pax7, Myf5, c-met, and M-cadherin. Immunostaining of a cytospin preparation of the sorted SM/C-2.6-positive cells showed that these cells were positive for M-cadherin (*C*), and Pax7 (*D*) (white arrowheads). Scale bars = 20 μm (*C*); 50 μm (*D*).

(both $P<0.05$; **Fig. 3**). Thus, ES-derived satellite-like cells isolated using the SM/C-2.6 antibody possess strong myogenic potential *in vitro*.

Damaged muscle can be repaired by transplantation of ES-derived satellite-like cells

To examine the myogenic potential of ES-derived satellite-like cells *in vivo*, SM/C-2.6-positive and -negative cells were transplanted into conditioned mdx mice (15). The LTA muscles of recipient mdx mice were preinjured with CTX (primary injury; ref. 30) 24 h prior to transplantation, and mice were exposed to 8 cGy of γ-irradiation (whole body) 12 h prior to transplantation (**Fig. 4*A***). GFP-positive ES cells were used as donor cells in this experiment. GFP$^+$ES-derived SM/C-2.6-positive and -negative cells were directly injected into the predamaged LTA muscles. The recipient mice were analyzed 3 wk post-transplantation. By fluorescence stereomicroscopy, GFP-positive tissues were clearly observed within the LTA muscles injected with SM/C-2.6-positive cells (Fig. 4*B* and **Table 1**). In contrast, no GFP-positive tissue was observed in muscles injected with SM/C-2.6-negative cells (Fig. 4*C*). These GFP-positive tissues were further confirmed by diaminobenzidine staining using anti-GFP and a peroxidase-conjugated secondary antibody (Supplemental Fig. 4) to exclude the possibility of autofluorescence of the muscle tissues. Immunostaining with anti-MHC confirmed that these GFP-positive tissues were mature skeletal myofibers (Fig. 4*D*). In addition, GFP/Pax7 double-positive cells were observed within the LTA muscles of the recipient mice (Fig. 4*E* and Supplemental Fig. 5) and in isolated single fibers (Fig. 4*F* and Table 1). The GFP-positive cells were also confirmed to be positive for other satellite cell markers such as Myf5 and M-cadherin (Supplemental Figs. 6 and 7). These GFP/Pax7-double-positive cells were located along the periphery of the muscle fascicle. With laminin immunostaining we verified that the location of the GFP-positive mononuclear cells was between the basal lamina and the muscle cell plasma membrane, a location consistent with the anatomical definition of satellite cells

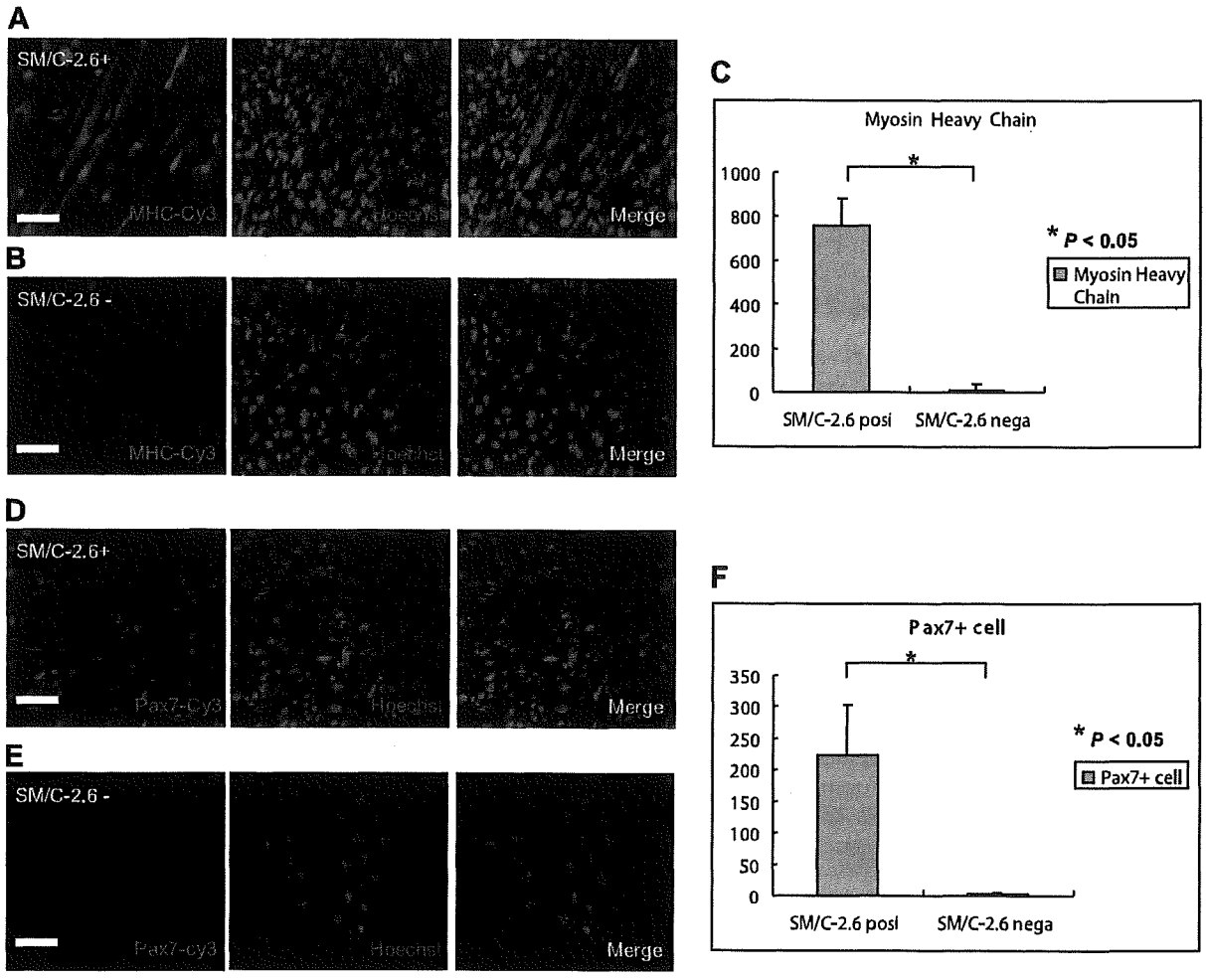

Figure 3. ES-derived satellite-like cells have strong myogenic potential *in vitro*. Immunostaining detected an abundant number of MHC-positive fibers and Pax7-positive cells in SM/C-2.6-positive cell culture (*A*, *D*) but not SM/C-2.6-negative cells (*B*, *E*) after 1 wk in culture. Scale bars = 50 μm. Significant differences were observed in the number of MHC-positive fibers and Pax7-positive cells per well between sorted SM/C-2.6-positive and -negative cell cultures (*C*, *F*).

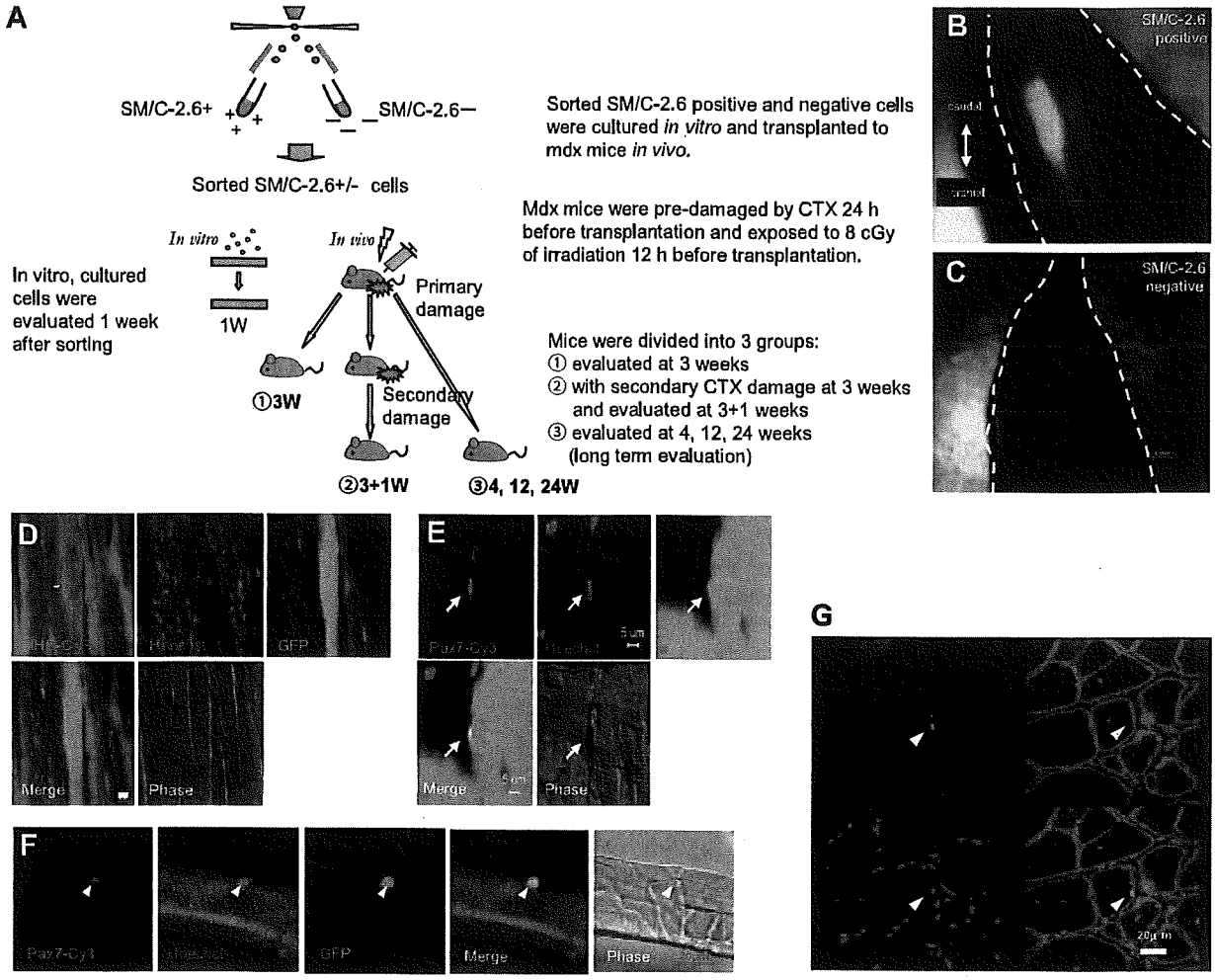

Figure 4. ES-derived satellite-like cells can repair damaged muscle *in vivo*. *A*) Methods for *in vitro* and *in vivo* analysis of sorted SM/C-2.6-positive and -negative cells derived from mES cells. *B, C*) ES-derived GFP-positive tissue engrafted to the LTA muscle of a recipient mouse that received SM/C-2.6-positive cells (*B*) but SM/C-2.6-negative cells (*C*). *D*) Grafted GFP-positive tissues were histologically MHC positive. *E*) GFP/Pax7-double-positive cells were observed in mice that received SM/C-2.6-positive cells by anti-Pax7 immunostaining. *F*) GFP/Pax7-double-positive cells were also confirmed by immunostaining of isolated single fibers. *G*) Laminin immunostaining indicated that the GFP-positive cells were located between the basal lamina and the muscle cell plasma membrane, which is consistent with the anatomical definition of muscle satellite cells. Scale bars = 1 mm (*B, C*); 15 μm (*D*); 5 μm (*E*); 20 μm (*F, G*).

(Fig. 4*G*). In contrast, in mice transplanted with SM/C-2.6-negative cells, GFP-positive tissues were rarely observed, and none of the GFP-positive cells were positive for skeletal MHC. H&E staining indicated that these GFP-positive tissues were surrounded by inflammatory cells (Supplemental Fig. 8), suggesting that these nonmyogenic tissues may undergo phagocytosis. These results demonstrate that ES-derived SM/C-2.6-positive satellite-like cells could be engrafted *in vivo* and repair damaged muscle tissues of the host.

Engrafted ES-derived satellite-like cells function as satellite cells following muscle damage

Muscle satellite cells are generally considered to be self-renewing monopotent stem cells that differentiate into myoblasts and myofibers to repair damaged skeletal muscles. To determine whether these engrafted GFP^+ES-derived satellite-like cells are functional stem cells, we injured the LTA muscle of primary recipient mice 3 wk after primary transplantation with GFP^+SM/C-2.6-positive cells. This experiment let us assess the ability of satellite-like cells to repair damaged muscle fibers and self-renew *in vivo* (14). The LTA muscles were removed and analyzed 1 wk after the secondary injury (reinjured group). Mice that were initially injected with GFP^+SM/C-2.6-positive cells without a second injury were used as a control (nonreinjured group). These control mice were analyzed 3 or 4 wk after transplantation (Fig. 4*A*). GFP-positive muscle fascicles were counted in sections of both reinjured and nonreinjured muscle (**Fig. 5*A, B***). In the reinjured group 461.7 ± 117.4 (n=6; per view, ×100) GFP-positive muscle fascicles were observed. In comparison, only 136.7 ± 27.9 (n=4) and 168.7 ± 72.9 (n=6; per view, ×100) GFP-positive muscle fascicles were evident in

TABLE 1. *Transplantation of reinjured and nonreinjured mice and long-term evaluation*

Group	TA with GFP$^+$ fascicles [n(%)]^a	Mouse	Cells/TA injected (n)	GFP$^+$ fascicles/TA (avg)^b	GFP$^+$/Pax7$^+$ cells/TA (avg)^c	Engraftment efficiency
SM/C-2.6$^+$						
3W	4/8 (50%)	1	1.75×10^4	125.3	5.3	
		2	3.5×10^4	111.1	7.1	
		3	5×10^4	134.2	5.1	
		4	8×10^4	176.1	4.2	
Mean			$4.5 \pm 2.6 \times 10^4$	136.7 ± 27.0	5.4 ± 1.2	0.30%
4W	6/9 (66.67%)	1	2×10^4	77.3	6.1	
		2	1.3×10^5	153.2	4.6	
		3	5×10^4	163.1	6.8	
		4	3.5×10^4	168.9	5.1	
		5	8×10^4	281.1	7.2	
		6	1.75×10^4	169.4	6.2	
Mean			$3.6 \pm 2.5 \times 10^4$	168.7 ± 72.9	6 ± 1	0.47%
3 + 1W	6/8 (75%)	1	2×10^4	581.2	11.2	
		2	1.3×10^5	370.3	11.5	
		3	5×10^4	586.6	10.1	
		4	3.5×10^4	486.6	5.9	
		5	8×10^4	347.1	15.3	
		6	1.75×10^4	542.9	10.8	
Mean			$5.5 \pm 4.3 \times 10^4$	461.7 ± 117.3	10.8 ± 3	0.84%
12W	3/5 (60%)	1	2×10^4	391.5	9.7	
		2	5×10^4	266	9.3	
		3	8×10^4	280.2	6	
Mean			$5 \pm 3 \times 10^4$	312.6 ± 68.7	8.3 ± 2	0.59%
24W	1/2 (50%)	1	2×10^4	58.62	3.45	
Mean			2×10^4	58.62	3.45	0.20%
SM/C-2.6$^-$						
3W	0/8 (0%)	1–8	$1–8 \times 10^4$	0	0	0%
4W	0/9 (0%)	1–9	$1.3–8 \times 10^4$	0	0	0%
3 + 1W	0/8 (0%)	1–8	$1.75–13 \times 10^4$	0	0	0%
12W	0/5 (0%)	1–8	$2–8 \times 10^4$	0	0	0%
24W	0/2 (0%)	1–2	2×10^4	0	0	0%

Serial transplantation

	Primary transplantation		Secondary transplantation		
Mouse	Cells injected	Collected GFP$^+$ cells/TA	Cells injected	GFP$^+$ fascicles/TA	Engraftment efficiency
1	2×10^4	3253	200	29.3	14.7%
2	2×10^4	2277	200	28.6	14.3%
Mean	2×10^4	2765	200	29 ± 0.5	14.5%

TA, tibialis anterior; 3W, nonreinjured group analyzed 3 wk after cell transplantation; 4W, nonreinjured group analyzed 4 wk after cell transplantation; 3 + 1W, reinjured group reinjured 3 wk after cell transplantation and analyzed 1 wk after reinjury; 12W, long-term engraftment evaluation analyzed 12 wk after cell transplantation; 24W, long-term engraftment evaluation analyzed 24 wk after cell transplantation. ^{a}Percentage of TA that had engrafted with GFP$^+$ fibers was calculated as number of TAs with GFP$^+$ fibers/total TAs injected with cells. ^{b}Average determined from number of GFP$^+$ muscle fascicles counted per field at ×100 in 10 fields. ^{c}Average determined from number of GFP$^+$/Pax7+ cells counted per field at ×100 in 10 fields.

the nonreinjured groups at 3 and 4 wk, respectively, after transplantation (Fig. 5*B* and Table 1). Furthermore, we also observed that many GFP-positive muscle fibers had a typical central nucleus in the reinjured group (Fig. 5*C*), indicating regenerating muscle fibers. Taken together, these results suggest that these GFP-positive muscle tubes were freshly regenerated by the engrafted GFP$^+$ ES-derived satellite-like cells in response to the second injury. Surprisingly, immunostaining with anti-Pax7 revealed an increase in number of GFP/Pax7-double-positive cells in the reinjured group (10.8±3.0/view compared to 5.4±1.2, and 6.0±1.0 in the nonreinjured group; Fig. 5*D* and Table 1). This result strongly suggests that engrafted ES-derived satellite-like cells not only self-renewed but also expanded in number, possibly replacing the recipient satellite cells lost because of excessive repair of skeletal muscle in response to the second injury.

ES-derived satellite-like cells are capable of long-term engraftment in recipient muscles

Long-term engraftment is an important characteristic of self-renewing stem cells. If these ES-derived satellite-

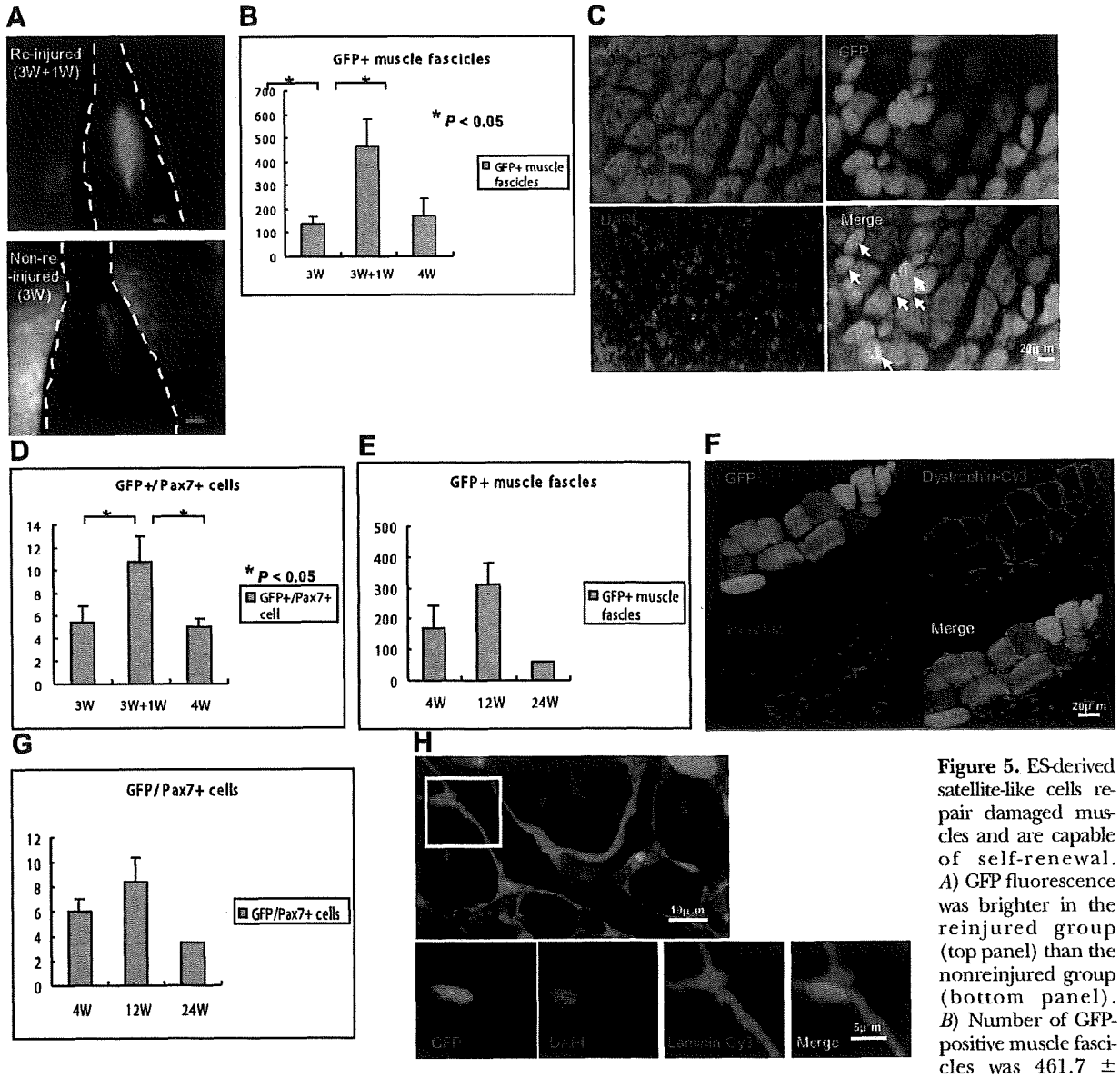

Figure 5. ES-derived satellite-like cells repair damaged muscles and are capable of self-renewal. *A*) GFP fluorescence was brighter in the reinjured group (top panel) than the nonreinjured group (bottom panel). *B*) Number of GFP-positive muscle fascicles was 461.7 ± 117.3 in the reinjured group (3W+1W) and 136.7 ± 27.9 and 168.7 ± 72.9 in the nonreinjured group at 3 wk (3W) and 4 wk (4W), respectively. *C*) GFP-positive fibers were confirmed to be MHC positive and contained central nuclei (arrows). *D*) Number of GFP/Pax7-double-positive cells also increased significantly in the reinjured group (10.8±3.0 cells at 3W+1W) compared to the nonreinjured group (5.4±1.2 and 6.0±1.0 at 3W and 4W, respectively). *E*) In long-term evaluations, number of GFP-positive muscle fascicles at 12 wk (12W) increased relative to number at 4 wk after transplantation [312.6±68.7 (n=3) *vs.* 168.7±72.9]. However, a decrease was observed at 24 wk (58.6; n=1). *F*) Immunostaining showed dystrophin (red) surrounding the donor-derived GFP-positive fibers (green), 24 wk after transplantation of SM/C-2.6-positive cells. *G*) Results similar to *E* were observed with the number of GFP/Pax7-double-positive cells. *H*) A GFP-positive cell beneath the basal lamina was observed. Scale bars = 1 mm (*A*); 20 μm (*C*); 20 μm (*F*); 10 μm (*H*, top panel); 5 μm (*H*, bottom panels).

like cells function as normal stem cells in skeletal muscle, they should be able to reside within the tissue for long periods of time and undergo asymmetric cell divisions to maintain the number of satellite cells and to generate muscle fibers. To examine this stem cell function, we analyzed the recipient mice at 4, 12, and 24 wk after transplantation. Intriguingly, in the LTA muscle of mdx mice transplanted with SM/C-2.6-positive cells, the number of GFP-positive fascicles at 12 wk increased over that at 4 wk [12.6±68.7 (n=3) *vs.* 168.7±72.9; Fig. 5*E*] but decreased by 24 wk (58.6; n=1). These engrafted GFP-positive tissues were confirmed to be MHC positive through immunostaining (Supplemental Fig. 9), and surrounding these GFP-positive fibers, dystrophin was observed (Fig. 5*F*). The numbers of GFP/Pax7-double-positive cells were maintained from week 4 to week 24 (Fig. 5*G*, Table 1, and Supplemental Fig. 10) and the location of GFP-positive cells under the basal lamina meets the anatomical definition of satellite cells (Fig. 5*H*). No teratomas were

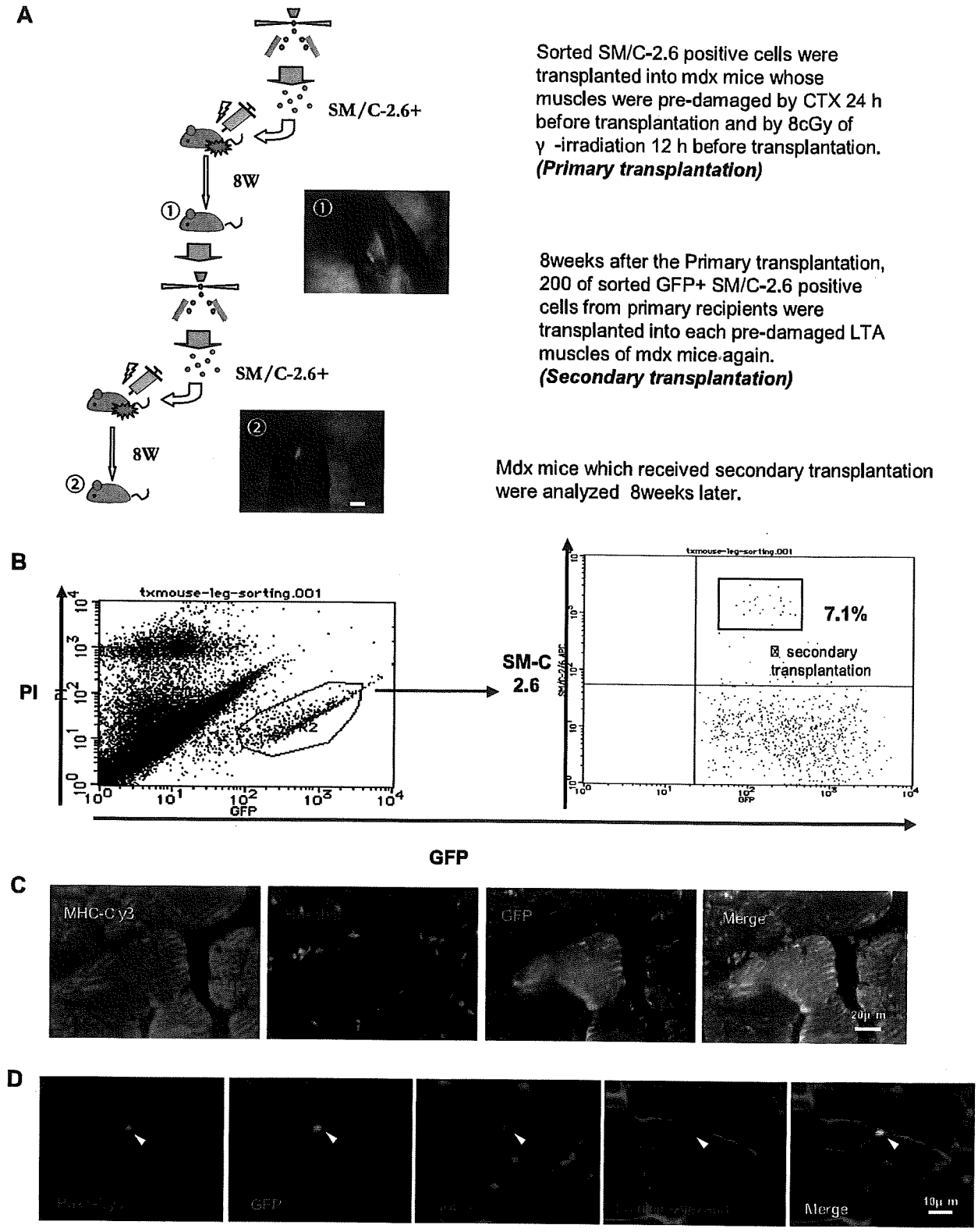

Figure 6. ES-derived satellite-like cells can be secondarily transplanted. *A*) SM/C-2.6-positive cells (2.5×10^4) were transplanted into the LTA muscle of recipient mice in primary transplantation, and as few as 200 SM/C-2.6-positive cells collected from the primary recipients were retransplanted (secondary transplantation) into the LTA muscle of secondary recipient mice. *B*) FACS data of primary transplantation indicated that 7.1% of engrafted (GFP-positive) cells were SM/C-2.6-positive. *C*) Eight weeks after secondary transplantation, immunostaining of LTA muscle for MHC showed that engrafted ES-derived GFP-positive tissues formed mature skeletal muscle fibers. *D*) GFP/Pax7-double-positive cells (arrowhead) located beneath the basal lamina were observed within GFP-positive LTA muscle of secondary recipient mice. Scale bars = 2 mm (*A*); 20 μm (*C*); 10 μm (*D*).

found in recipient mice transplanted with SM/C-2.6-positive cells. Thus, ES-derived satellite-like cells effectively engrafted and provided long-term stem cells, which played an important role in maintenance of the integrity of the surrounding muscle tissue.

ES-derived satellite-like cells can be secondarily transplanted

For a more thorough characterization of the ES-derived satellite-like cells, we performed serial transplantations. Eight weeks after the primary cell transplantation with 2×10^4 SM/C-2.6-positive cells, the LTA muscles of the primary recipient mice were dissected to isolate the engrafted ES-derived cells, 2765 ± 685.9 (n=2; **Fig. 6*A***). The GFP^+/SM/C-2.6-positive cells within the engrafted cells were sorted by FACS (204±33.9; n=2), and only 200 GFP+/SM/C-2.6-positive cells/mouse were transplanted into predamaged LTA muscles of mdx mice (Fig. 6*B*). Eight weeks later (16 wk after the primary transplantation), the recipient mice were analyzed. GFP-positive tissue in the LTA muscle of the secondary recipient mice was observed (Fig. 6*A*). The GFP-positive tissues were confirmed to be MHC-positive mature skeletal muscle (Fig. 6*C*), and surrounding these engrafted GFP-positive skeletal muscle fascicles, dystrophin was observed (Supplemental Fig. 11). GFP/Pax7-double-positive cells located beneath the basal lamina were also detected in the engrafted tissue (Fig. 6*D*). Thus, with only 200 GFP^+SMC/2.6-positive cells, injured skeletal muscle and Pax7+ cells were successfully restored in the secondary recipients. These findings demonstrate that stem cell fraction contained within SM/C-2.6-positive cells was enriched *in vivo* through transplantation.

DISCUSSION

Many attempts have been made to induce mES cells into the skeletal muscle lineage, with hanging drop cultures for EB formation being the most widely applied method (25). However, although EBs contain cells derived from all 3 germ layers, effective induction of mES cells into the myogenic lineage, including myogenic stem cells (satellite cells), has not yet been achieved. Because of the lack of adequate surface markers, purifying ES-derived myogenic precursor/stem cells from differentiated mES cells *in vitro* has been difficult. To overcome these problems, we modified the classic EB culture system by combining it with aspects of the single-fiber culture method. Single-fiber culture (33) has been used for functional evaluation of satellite cells. When a single myofiber is plated on a Matrigel-coated plate with DMEM containing HS, satellite cells migrate out of the fiber and differentiate into myoblasts to form myofibers *in vitro*. Matrigel allows the migrating satellite cells to proliferate before differentiating and fusing into large multinucleated myotubes (35). We hypothesized that this Matrigel environment might be suitable for ES cell differentiation into satellite cells and myoblasts. Therefore, we introduced Matrigel and HS into the classic EB culture system and established an efficient induction system for myogenic lineage cells, including cells expressing Pax7, a commonly recognized marker for skeletal muscle stem cells. Furthermore, we also successfully enriched ES-derived Pax7-positive myogenic precursor/stem cells using the SM/C-2.6 antibody.

The steps in ES cell induction are thought to be homologous to normal embryogenesis. During normal skeletal myogenesis, the initial wave of myogenic precursor cells in the dermomyotome express Myf5/MRF4 and Pax3, followed by a wave of Pax3/Pax7 expression (36). These waves of myogenesis act upstream of the primary myogenic transcription factor MyoD (37-39). In myotome formation skeletal myogenesis begins with myoblasts, termed somitic myoblasts, which appear at approximately E8.5, followed by the appearance of embryonic myoblasts (E11.5), fetal myoblasts (E16.5), and, ultimately, satellite cells, which are responsible for postnatal muscle regeneration (40). Our RT-PCR results (Fig. 1*J*) showed an earlier appearance of Pax3 expression, on d 3 + 3, followed by Pax3/Pax7 expression on d 3 + 3 + 7 and stronger expression of Pax3 than Pax7. These results resemble normal myogenesis, in which the primary wave of myogenesis is followed by a secondary wave of Pax3/Pax7-dependent myogenesis (41). Considering that in the time course of myogenesis satellite cells emerge during late fetal development, ES-derived Pax7-positive cells were collected on d 3 + 3 + 14 in an attempt to acquire cells that correspond to those of the late fetal to neonatal period. However, RT-PCR results of myogenic factors in SM/C-2.6-positive cells (Fig. 2*B*) indicated that these ES-derived SM/C-2.6-positive cells are a heterogeneous population, because they express not only Pax3 and Pax7 but also Myf5 and c-met. Although further confirmation is needed, we hypothesize that both embryonic/fetal myoblasts expressing Myf-5 and/or c-met and satellite/long-term stem cells expressing Pax3/Pax7 are present.

To confirm that the ES-derived SM/C-2.6-positive cell population contained functional satellite cells, the muscle regeneration and self-renewal capacities were examined. Recently Collins *et al.* established an excellent system in which sequential damage to the muscle of a recipient mouse was applied, to evaluate both muscle regeneration and self-renewal (14) Using their experimental approach, a significant increase in numbers of both ES-derived GFP-positive muscle fascicles and GFP/Pax7-double-positive cells was observed in mice that received a second injury. This result not only demonstrates the myogenic ability of ES-derived cells but also strongly supports the idea that these cells undergo self-renewal *in vivo*.

Analysis of long-term engraftment is an important method to verify self-renewal ability, for 2 reasons. First, ES-derived satellite cells must be able to engraft for long periods of time in order to provide the amount of progeny needed for repairing damaged tissue for an

extended period. In our study the ES-derived GFP-positive skeletal muscle tissues and Pax7-positive cells engrafted up to 24 wk and were located beneath the basal lamina, which is consistent with the anatomical definition of satellite cells. Although the number of GFP-positive fascicles at 24 wk decreased compared to 12 wk, this diminution may be due to the heterogeneity of ES-derived SM/C-2.6-positive cells as we mentioned. Because myoblasts cannot support myogenesis in the long term, we believe that GFP-positive fascicles at 24 wk are products of ES-derived satellite-like cells. Second, one of the potential risks of ES cell transplantation is teratoma formation. Considering clinical applications, it is extremely important to prevent formation of teratomas in the recipients. In our study more than 60 transplanted mice were evaluated through gross morphological and histological examination. There were no teratomas formed in mice that received SM/C-2.6-positive cells, and only 1 teratoma was found among the mice that received SM/C-2.6-negative cells. This result suggests that the risk of tumor formation by the ES cells was eliminated by using sorted SM/C-2.6-positive cells.

In addition to the sequential damage model and the long-term engraftment evaluation, we performed serial transplantations to further confirm the stem cell properties of these ES-derived SM/C-2.6-positive cells. Serial transplantation enables the identification and separation of long-term stem cells from short-term progenitors (42). To eliminate myoblast involvement, we designed a serial transplantation protocol of 8 + 8 wk (*i.e.*, a second transplantation 8 wk after the primary transplantation and an analysis of recipient mice 8 wk after the second transplantation). Strikingly these recollected ES-derived SM/C-2.6-positive cells showed significantly higher engraftment efficiency compared to the primary transplantation. In the previous reports engraftment efficiencies of myoblasts transplantation was ~0.1-0.2%, with the highest reported value being 2% (43-45). This engraftment efficiency is similar to our primary transplantation (0.2-0.8%) as well as the plating efficiency of SM/C-2.6-positive cells *in vitro* (0.07%). In our study as few as 200 recollected ES-derived SM/C-2.6-positive cells were transplanted in the second transplantation, and 29.0 ± 0.47 (n=2) fascicles were observed, which indicates 14.7% of higher engraftment efficiency. Thus, through the serial transplantation, ES-derived stem cell fraction was purified. A comparison of these SM/C-2.6-positive cells before and after injection might help to characterize the stem cell fraction derived from ES cells.

There have been few reports describing transplantation of ES-derived myogenic cells into injured muscles, and the report of engraftable skeletal myoblasts derived from human ES cells represents significant progress (26). Recently Darabi *et al.* (46) have reported that by introducing Pax3 into mouse embryoid bodies, autonomous myogenesis was initiated *in vitro*, and Pax3-induced cells regenerated skeletal muscles *in vivo* by sorting the PDGF-a+Flk-1- cells. The Pax3 expression was not observed until 7 d of differentiation culture, but introduced Pax3 expression pushed EBs to myogenic differentiation. Interestingly, we observed Pax3 expression at d 3 + 3 weakly and d 3 + 3 + 7 strongly, and gene expression process in our culture is very similar to theirs. In prolonged culture using Matrigel and HS, EBs were able to initiate myogenesis without gene modification in our system.

In conclusion, we successfully generated transplantable myogenic cells, including satellite-like cells, from mES cells. The ES-derived myogenic precursor/stem cells could be enriched using a novel antibody, SM/C-2.6. These ES-derived SM/C-2.6-positive cells possess a high myogenic potential, participate in muscle regeneration, and are located beneath the basal lamina where satellite cells normally reside. The self-renewal of these ES-derived satellite-like cells enabled them to survive long-term engraftment, up to 24 wk. Through serial transplantation, these ES-derived SM/C-2.6-positive cells were further enriched and produced a high engraftment efficiency of 14.7%.

Our success in inducing mES cells to form functional muscle stem cells, the satellite-like cells, will provide an important foundation for clinical applications in the treatment of DMD patients. FJ

This work was supported by a Grant-in-Aid for Scientific Research (S) (19109006) and a Grant-in-Aid for Scientific Research (B) (18390298) from the Ministry of Education, Science, Technology, Sports, and Culture of Japan.

REFERENCES

1. Nawrotzki, R., Blake, D. J., and Davies, K. E. (1996) The genetic basis of neuromuscular disorders. *Trends Genet.* **12,** 294–298
2. Emery, A. E. (2002) The muscular dystrophies. *Lancet* **359,** 687–695
3. Michalak, M., and Opas, M. (1997) Functions of dystrophin and dystrophin associated proteins. *Curr. Opin. Neurol.* **10,** 436–442
4. Suzuki, A., Yoshida, M., Hayashi, K., Mizuno, Y., Hagiwara, Y., and Ozawa, E. (1994) Molecular organization at the glycoprotein-complex-binding site of dystrophin. Three dystrophin-associated proteins bind directly to the carboxy-terminal portion of dystrophin. *Eur. J. Biochem./FEBS* **220,** 283–292
5. Bonilla, E., Samitt, C. E., Miranda, A. F., Hays, A. P., Salviati, G., DiMauro, S., Kunkel, L. M., Hoffman, E. P., and Rowland, L. P. (1988) Duchenne muscular dystrophy: deficiency of dystrophin at the muscle cell surface. *Cell* **54,** 447–452
6. Mauro, A. (1961) Satellite cell of skeletal muscle fibers. *J. Biophys. Biochem. Cytol.* **9,** 493–495
7. Moss, F. P., and Leblond, C. P. (1971) Satellite cells as the source of nuclei in muscles of growing rats. *Anat. Rec.* **170,** 421–435
8. Snow, M. H. (1978) An autoradiographic study of satellite cell differentiation into regenerating myotubes following transplantation of muscles in young rats. *Cell Tissue Res.* **186,** 535–540
9. Jejurikar, S. S., and Kuzon, W. M., Jr. (2003) Satellite cell depletion in degenerative skeletal muscle. *Apoptosis* **8,** 573–578
10. Schultz, E., and Jaryszak, D. L. (1985) Effects of skeletal muscle regeneration on the proliferation potential of satellite cells. *Mech. Ageing Dev.* **30,** 63–72
11. Webster, C., and Blau, H. M. (1990) Accelerated age-related decline in replicative life-span of Duchenne muscular dystrophy myoblasts: implications for cell and gene therapy. *Somat. Cell Mol. Genet.* **16,** 557–565
12. Hashimoto, N., Murase, T., Kondo, S., Okuda, A., and Inagawa-Ogashiwa, M. (2004) Muscle reconstitution by muscle satellite

cell descendants with stem cell-like properties. *Development (Camb.)* **131,** 5481–5490
13. Montarras, D., Morgan, J., Collins, C., Relaix, F., Zaffran, S., Cumano, A., Partridge, T., and Buckingham, M. (2005) Direct isolation of satellite cells for skeletal muscle regeneration. *Science* **309,** 2064–2067
14. Collins, C. A., Olsen, I., Zammit, P. S., Heslop, L., Petrie, A., Partridge, T. A., and Morgan, J. E. (2005) Stem cell function, self-renewal, and behavioral heterogeneity of cells from the adult muscle satellite cell niche. *Cell* **122,** 289–301
15. Partridge, T. A., Morgan, J. E., Coulton, G. R., Hoffman, E. P., and Kunkel, L. M. (1989) Conversion of mdx myofibres from dystrophin-negative to -positive by injection of normal myoblasts. *Nature* **337,** 176–179
16. Mendell, J. R., Kissel, J. T., Amato, A. A., King, W., Signore, L., Prior, T. W., Sahenk, Z., Benson, S., McAndrew, P. E., Rice, R., Nagaraja, H., Stephens, R., Lantry, L., Morris, G. E., and Burghes, A. H. M. (1995) Myoblast transfer in the treatment of Duchenne's muscular dystrophy. *N. Engl. J. Med.* **333,** 832–838
17. Weissman, I. L., Anderson, D. J., and Gage, F. (2001) Stem and progenitor cells: origins, phenotypes, lineage commitments, and transdifferentiations. *Annu. Rev. Cell Dev. Biol.* **17,** 387–403
18. Relaix, F., Montarras, D., Zaffran, S., Gayraud-Morel, B., Rocancourt, D., Tajbakhsh, S., Mansouri, A., Cumano, A., and Buckingham, M. (2006) Pax3 and Pax7 have distinct and overlapping functions in adult muscle progenitor cells. *J. Cell Biol.* **172,** 91–102
19. Seale, P., Sabourin, L. A., Girgis-Gabardo, A., Mansouri, A., Gruss, P., and Rudnicki, M. A. (2000) Pax7 is required for the specification of myogenic satellite cells. *Cell* **102,** 777–786
20. Cornelison, D. D., and Wold, B. J. (1997) Single-cell analysis of regulatory gene expression in quiescent and activated mouse skeletal muscle satellite cells. *Dev. Biol.* **191,** 270–283
21. Hollnagel, A., Grund, C., Franke, W. W., and Arnold, H. H. (2002) The cell adhesion molecule M-cadherin is not essential for muscle development and regeneration. *Mol. Cell. Biol.* **22,** 4760–4770
22. Bottaro, D. P., Rubin, J. S., Faletto, D. L., Chan, A. M., Kmiecik, T. E., Vande Woude, G. F., and Aaronson, S. A. (1991) Identification of the hepatocyte growth factor receptor as the c-met proto-oncogene product. *Science* **251,** 802–804
23. Fukada, S., Higuchi, S., Segawa, M., Koda, K., Yamamoto, Y., Tsujikawa, K., Kohama, Y., Uezumi, A., Imamura, M., Miyagoe-Suzuki, Y., Takeda, S., and Yamamoto, H. (2004) Purification and cell-surface marker characterization of quiescent satellite cells from murine skeletal muscle by a novel monoclonal antibody. *Exp. Cell Res.* **296,** 245–255
24. Dekel, I., Magal, Y., Pearson-White, S., Emerson, C. P., and Shani, M. (1992) Conditional conversion of ES cells to skeletal muscle by an exogenous MyoD1 gene. *New Biol.* **4,** 217–224
25. Rohwedel, J., Maltsev, V., Bober, E., Arnold, H. H., Hescheler, J., and Wobus, A. M. (1994) Muscle cell differentiation of embryonic stem cells reflects myogenesis in vivo: developmentally regulated expression of myogenic determination genes and functional expression of ionic currents. *Dev. Biol.* **164,** 87–101
26. Barberi, T., Bradbury, M., Dincer, Z., Panagiotakos, G., Socci, N. D., and Studer, L. (2007) Derivation of engraftable skeletal myoblasts from human embryonic stem cells. *Nat. Med.* **13,** 642–648
27. Doetschman, T. C., Eistetter, H., Katz, M., Schmidt, W., and Kemler, R. (1985) The in vitro development of blastocyst-derived embryonic stem cell lines: formation of visceral yolk sac, blood islands and myocardium. *J. Embryol. Exp. Morphol.* **87,** 27–45
28. Niwa, H., Yamamura, K., and Miyazaki, J. (1991) Efficient selection for high-expression transfectants with a novel eukaryotic vector. *Gene* **108,** 193–199
29. Yoshimoto, M., Chang, H., Shiota, M., Kobayashi, H., Umeda, K., Kawakami, A., Heike, T., and Nakahata, T. (2005) Two different roles of purified CD45+c-Kit+Sca-1+Lin- cells after transplantation in muscles. *Stem Cells (Dayton)* **23,** 610–618
30. Harris, J. B. (2003) Myotoxic phospholipases A2 and the regeneration of skeletal muscles. *Toxicon* **42,** 933–945
31. Fukada, S., Miyagoe-Suzuki, Y., Tsukihara, H., Yuasa, K., Higuchi, S., Ono, S., Tsujikawa, K., Takeda, S., and Yamamoto, H. (2002) Muscle regeneration by reconstitution with bone marrow or fetal liver cells from green fluorescent protein-gene transgenic mice. *J. Cell Sci.* **115,** 1285–1293
32. Gross, J. G., and Morgan, J. E. (1999) Muscle precursor cells injected into irradiated mdx mouse muscle persist after serial injury. *Muscle Nerve* **22,** 174–185
33. Rosenblatt, J. D., Lunt, A. I., Parry, D. J., and Partridge, T. A. (1995) Culturing satellite cells from living single muscle fiber explants. *In Vitro Cell. Dev. Biol.* **31,** 773–779
34. Dhawan, J., and Rando, T. A. (2005) Stem cells in postnatal myogenesis: molecular mechanisms of satellite cell quiescence, activation and replenishment. *Trends Cell Biol.* **15,** 666–673
35. Zammit, P. S., Relaix, F., Nagata, Y., Ruiz, A. P., Collins, C. A., Partridge, T. A., and Beauchamp, J. R. (2006) Pax7 and myogenic progression in skeletal muscle satellite cells. *J. Cell Sci.* **119,** 1824–1832
36. Relaix, F., Rocancourt, D., Mansouri, A., and Buckingham, M. (2005) A Pax3/Pax7-dependent population of skeletal muscle progenitor cells. *Nature* **435,** 948–953
37. Tajbakhsh, S., Rocancourt, D., Cossu, G., and Buckingham, M. (1997) Redefining the genetic hierarchies controlling skeletal myogenesis: Pax-3 and Myf-5 act upstream of MyoD. *Cell* **89,** 127–138
38. Kiefer, J. C., and Hauschka, S. D. (2001) Myf-5 is transiently expressed in nonmuscle mesoderm and exhibits dynamic regional changes within the presegmented mesoderm and somites I-IV. *Dev. Biol.* **232,** 77–90
39. Hirsinger, E., Malapert, P., Dubrulle, J., Delfini, M. C., Duprez, D., Henrique, D., Ish-Horowicz, D., and Pourquie, O. (2001) Notch signalling acts in postmitotic avian myogenic cells to control MyoD activation. *Development (Camb.)* **128,** 107–116
40. Smith, T. H., Block, N. E., Rhodes, S. J., Konieczny, S. F., and Miller, J. B. (1993) A unique pattern of expression of the four muscle regulatory factor proteins distinguishes somitic from embryonic, fetal and newborn mouse myogenic cells. *Development (Camb.)* **117,** 1125–1133
41. Kassar-Duchossoy, L., Giacone, E., Gayraud-Morel, B., Jory, A., Gomes, D., and Tajbakhsh, S. (2005) Pax3/Pax7 mark a novel population of primitive myogenic cells during development. *Genes Dev.* **19,** 1426–1431
42. Harrison, D. E., Astle, C. M., and Delaittre, J. A. (1978) Loss of proliferative capacity in immunohemopoietic stem cells caused by serial transplantation rather than aging. *J. Exp. Med.* **147,** 1526–1531
43. Yao, S. N., and Kurachi, K. (1993) Implanted myoblasts not only fuse with myofibers but also survive as muscle precursor cells. *J. Cell Sci.* **105**(Pt. 4), 957–963
44. Rando, T. A., and Blau, H. M. (1994) Primary mouse myoblast purification, characterization, and transplantation for cell-mediated gene therapy. *J. Cell Biol.* **125,** 1275–1287
45. Sherwood, R. I., Christensen, J. L., Conboy, I. M., Conboy, M. J., Rando, T. A., Weissman, I. L., and Wagers, A. J. (2004) Isolation of adult mouse myogenic progenitors: functional heterogeneity of cells within and engrafting skeletal muscle. *Cell* **119,** 543–554
46. Darabi, R., Gehlbach, K., Bachoo, R. M., Kamath, S., Osawa, M., Kamm, K. E., Kyba, M., and Perlingeiro, R. C. (2008) Functional skeletal muscle regeneration from differentiating embryonic stem cells. *Nat. Med.* **14,** 134–143

Received for publication October 21, 2008.
Accepted for publication January 8, 2009.

Direct Hematological Toxicity and Illegitimate Chromosomal Recombination Caused by the Systemic Activation of CreER^{T2} [1]

Atsuko Yoshioka Higashi,* Tomokatsu Ikawa,[¶] Masamichi Muramatsu,[‖] Aris N. Economides,[#] Akira Niwa,[†] Tomohiko Okuda,[‡] Andrew J. Murphy,[#] Jose Rojas,[#] Toshio Heike,[†] Tatsutoshi Nakahata,[†] Hiroshi Kawamoto,[¶] Toru Kita,* and Motoko Yanagita[2§]

The CreER^{T2} for conditional gene inactivation has become increasingly used in reverse mouse genetics, which enables temporal regulation of Cre activity using a mutant estrogen binding domain (ER^{T2}) to keep Cre inactive until the administration of tamoxifen. In this study, we present the severe toxicity of ubiquitously expressed CreER^{T2} in adult mice and embryos. The toxicity of Cre recombinase or CreER^{T2} in vitro or in vivo organisms are still less sufficiently recognized considering the common use of Cre/*loxP* system, though the toxicity might compromise the phenotypic analysis of the gene of interest. We analyzed two independent lines in which CreER^{T2} is knocked-in into the Rosa26 locus (R26CreER^{T2} mice), and both lines showed thymus atrophy, severe anemia, and illegitimate chromosomal rearrangement in hematopoietic cells after the administration of tamoxifen, and demonstrated complete recovery of hematological toxicity in adult mice. In the hematopoietic tissues in R26CreER^{T2} mice, reduced proliferation and increased apoptosis was observed after the administration of tamoxifen. Flow cytometric analysis revealed that CreER^{T2} toxicity affected several hematopoietic lineages, and that immature cells in these lineages tend to be more sensitive to the toxicity. In vitro culturing of hematopoietic cells from these mice further demonstrated the direct toxicity of CreER^{T2} on growth and differentiation of hematopoietic cells. We further demonstrated the cleavage of the putative cryptic/pseudo *loxP* site in the genome after the activation of CreER^{T2} in vivo. We discussed how to avoid the misinterpretation of the experimental results from potential toxic effects due to the activated CreER^{T2}. *The Journal of Immunology,* 2009, 182: 5633–5640.

Conditional gene inactivation using the Cre/*loxP* system has become increasingly used in reverse mouse genetics (1–6). This system takes advantage of the bacteriophage P1 Cre-recombinase ability to catalyze the excision of a DNA sequence flanked by *loxP* sequences. Inactivation of the target gene in conditional knockout mice is regulated depending on the expression pattern of Cre recombinase under the control of tissue-specific promoters (7, 8). However, to analyze gene functions in adult mice, additional temporal control of gene inactivation is indispensable to circumvent problems such as embryonic lethality or developmental abnormalities arising from the early onset of Cre recombinase activity.

Recently, temporal regulation of Cre recombinase activity has been accomplished using tetracycline-controlled gene expression and IFN-inducible expression (9, 10). Another approach uses engineered recombinase fused to the mutated ligand-binding domain of the estrogen receptor (ER^{T2}),[3] which does not bind endogenous estradiol but is highly sensitive to the synthetic ligand tamoxifen (TM) or its metabolite 4-hydroxytamoxifen (11). The fusion protein is inactivated by binding to heat shock proteins, until the administration of TM, when it is released from the complex, becomes active and excises *loxP*-flanked DNA regions. Several transgenic mouse lines have been generated that express CreER^{T2} fusion genes under the control of tissue-specific promoters, which show ligand-dependent recombination in certain cell types (12–17).

It has long been assumed that the expression of Cre recombinase does not adversely affect the physiology of the host cell, despite several reports alarming the toxicity of Cre recombinase. High levels of Cre expression have been reported to be toxic in some mammalian cells. Mouse embryonic fibroblasts, NIH3T3 cells, and some human cell lines can be sensitive to the continuous presence of Cre (18–20). Regarding the adverse effect of Cre in vivo, aberrant chromosomal rearrangement in spermatids and male

*Department of Cardiovascular Medicine, [†]Department of Pediatrics, [‡]COE Formation, [§]Career-Path Promotion Unit for Young Life Scientists, Graduate School of Medicine, Kyoto University, Kyoto, Japan; [¶]Laboratory for Lymphocyte Development, RIKEN Research Center for Allergy and Immunology, Yokohama, Japan; [‖]Department of Molecular Genetics, Graduate School of Medical Science, Kanazawa University, Kanazawa, Japan; and [#]Regeneron Pharmaceuticals, Tarrytown, NY 10591

Received for publication July 23, 2008. Accepted for publication February 26, 2009.

The costs of publication of this article were defrayed in part by the payment of page charges. This article must therefore be hereby marked *advertisement* in accordance with 18 U.S.C. Section 1734 solely to indicate this fact.

[1] This study was supported by Grants-in Aid from the Ministry of Education, Culture, Science, Sports, and Technology of Japan (Wakate 177090551, Ho-ga 19659219); a Center of Excellence grant from the Ministry of Education, Culture, Science, Sports, and Technology of Japan; a research grant for health sciences from the Japanese Ministry of Health, Labor, and Welfare; a grant from the Astellas Foundation for Research on Metabolic Disorders; a grant from the Novartis Foundation for the promotion of science; a grant from Kato Memorial Trust for Nambyo Research; a grant from Hayashi Memorial Foundation for Female Natural Scientists; a grant from Japan Foundation for Applied Enzymology; and in part by a grant-in-aid for Research on Biological Markers for New Drug Development, Health and Labour Sciences, Research Grants from the Ministry of Health, Labour and Welfare of Japan.

A.Y.H., T.I., A.N., T.O., and H.K. performed experiments; A.N.E., A.J.M., and J.R. generated R26CreER^{T2} mice; M.M., T.H., T.N., T.K., and M.Y. analyzed results and made the figures; and M.Y., M.M., and H.K. designed the research and wrote the paper.

[2] Address correspondence and reprint requests to M. Yanagita, Career-Path Promotion Unit for Young Life Scientists, Graduate School of Medicine, Kyoto University, Kyoto, Japan. E-mail address: motoy@kuhp.kyoto-u.ac.jp

[3] Abbreviations used in this paper: ER^{T2}, mutated ligand-binding domain of the estrogen receptor; TM, tamoxifen; WT, wild type; 4-OHT, 4-hydroxytamoxifen.

www.jimmunol.org/cgi/doi/10.4049/jimmunol.0802413

infertility has been reported in transgenic mice expressing Cre in postmeiotic spermatids (21). Another group reported dilated cardiomyopathy in their transgenic mice expressing Cre under the control of α-myosin H chain (22). Glucose impairment was also reported in commonly used transgenic mice expressing Cre under the control of the insulin 2 promoter (23).

CreER^{T2} was first expected to avoid adverse effects of Cre recombinase by keeping Cre recombinase inactive until the administration of TM. However, very recently, Naiche et al. (24) reported that systemic activation of CreER^{T2} results in lethal anemia and widespread apoptosis in embryos. In their report however, it is unclear whether the toxicity is the direct effect of CreER^{T2} or not.

In this study, we demonstrated widespread hematological toxicity of ubiquitously expressed CreER^{T2} in adult mice as well as in embryos. We analyzed two independent mouse lines in which CreER^{T2} is inserted into the R26 locus (R26CreER^{T2} mice), and both lines showed reduced proliferation, increased apoptosis, and illegitimate chromosomal rearrangement in hematopoietic cells after the administration of TM possibly due to the toxicity of CreER^{T2}. Flow cytometric analysis revealed that CreER^{T2} toxicity affected several hematopoietic lineages, and that immature cells in these lineages tend to be more sensitive to the toxicity. In vitro culturing of hematopoietic cells from these mice further demonstrated the direct toxicity of CreER^{T2} on growth and differentiation of hematopoietic cells. We further demonstrated the in vivo cleavage of the putative cryptic/pseudo *loxP* site in the genome after the activation of CreER^{T2}, which results in the illegitimate chromosomal rearrangement. These results emphasize the critical importance of including control mice carrying the Cre gene to avoid the misinterpretation of the results.

We further demonstrated that these hematological abnormalities in adult R26CreER^{T2} mice recover spontaneously after 1 mo, which ensures the availability of this mice in reverse mouse genetics provided appropriate control mice are included.

Materials and Methods

Animal use

One line of R26CreER^{T2} mice was purchased from ARTEMIS Pharmaceuticals (17). Another line of R26CreER^{T2} mice was generated by Regeneron Pharmaceuticals using Velocigene technology (25), essentially as described. The R26 locus was heterozygous for the CreER^{T2} knock-in in all experiments. Both lines were derived on a mixed 129/Svj and C57BL/6J background, and the contribution of 129/Svj was the same in every experiment. R26R Cre reporter mice (R26R mice) (26) were purchased from The Jackson Laboratory. All animal experiments were performed in accordance with the Institutional Guidelines, and were in accordance with National Institutes of Health guidelines.

Administration of TM

TM (Sigma-Aldrich) was dissolved in a sunflower oil/ethanol (9/1) mixture at 3.0 mg/ml. In adult R26CreER^{T2} mice at 8 to 12 wk, 35 mg/kg or 175 mg/kg TM was administered orally for indicated days depending on the experiments. One to four days later depending on experiments, mice were sacrificed and subjected to experiments. Wild-type (WT) littermates administered with the same amount of TM were used as controls. For R26CreER^{T2} embryos, 200 mg/kg TM was administered i.p. into pregnant mothers at E14.5, or 150 mg/kg TM was administered at both E13.5 and E14.5 depending on the experiments.

Antibodies

The following Abs were used: anti-Ter119, anti-Mac1 (M1/70), anti-Gr-1 (RB6-8C5), anti-B220 (RA3-6B2), anti-CD19 (1D3), anti-IgM (R6-60.2), anti-CD3 (145-2C11), anti-CD4 (L3T4), anti-CD8 (Ly2), anti-CD25 (PC61), and anti-c *kit* (2B8) were obtained from BD Pharmingen. Anti-Ter119, anti-Mac1, anti-Gr-1, anti-B220, anti-NK1.1, anti-CD3, anti-CD4, and anti-CD8, were used as Lin markers. Anti-Ter119 (BD Pharmingen) and anti-Ki67 (Novocastra) Abs were used for immunostaining.

Histological studies

The organs were fixed in Tris-buffered 10% formalin solution and embedded in paraffin. Sections (2 μm) were stained with H&E. β-gal staining was performed as previously described (27). For immunostaining, the specimens were fixed in 4% paraformaldehyde at 4°C overnight, serially soaked in 10, 20, and 30% sucrose/PBS and embedded in OCT compound (Tissue Tek, Sakura Finetech) and 6-μm sections were prepared. The sections were immunostained as previously described (28–30).

TUNEL staining

Sections were subjected to the TUNEL staining using the in situ apoptosis detection TUNEL kit (MK500, Takara) and visualized by reaction with 3,3′-diaminobenzidine (SK-4100; Vector) for 1 min.

Coculture of hematolopoietic cells with stromal cells

To assess the effect of CreER^{T2} activation on the differentiation of hematopoetic stem cells, Lin$^-$c-*kit*$^+$ cells were collected from the bone marrow of R26CreER^{T2} mice and WT littermates, cultured on a monolayer of TSt-4 cells (31), and administered with 1 μM of 4-OHT (Sigma-Aldrich) at various time points. We analyzed the differentiation of the Lin$^-$c-*kit*$^+$ cells by examining the expression of Ter119 for erythroid potential, CD19 for B cell potential, and Mac-1 for myeloid potential. To assess the effect of CreER^{T2} activation on the proliferation of differentiated hematopoetic cells, Mac-1$^+$ cells, and CD19$^+$ cells were collected, cocultured with TSt-4 cells, and administered with 4-OHT.

Chromosomal number and karyotype analysis

R26CreER^{T2} mice and WT littermates were treated with vehicle or TM for 5 consecutive days, and were sacrificed 3 days after the last administration. Bone marrow cells of these mice were cultured and chosen randomly for chromosomal number analysis (47 cells for R26CreER^{T2} mice treated with TM, 20 cells for WT mice treated with TM, and 50 cells for R26CreER^{T2} mice treated with vehicle) and for karyotype analysis (14 cells for R26CreER^{T2} mice treated with TM, 4 cells for WT mice treated with TM, and 7 cells for R26CreER^{T2} mice treated with vehicle) as previously described (32).

Quantification of rearranged cryptic loxP site in the genome by real-time PCR

Primers were designed around the candidate locus for cryptic/pseudo *loxP* site to detect the amount of intact genome. Sequences for primers were described in corresponding figure legend. Real-time PCR was performed with a 7700 Sequence Detection System (Applied Biosystems) using SYBR Green PCR amplification reagent (Applied Biosystems), and the results were normalized with the amount of GAPDH genome.

Statistical analysis

Data are presented as means ± SD. Statistical significance was assessed by nonpaired, nonparametric Student's *t* test.

Results

Systemic recombination in adult and embryo R26CreER^{T2} mice

First, we tested the recombination efficiency of R26CreER^{T2} mice using R26R Cre reporter mice (26) (R26R mice), which express *lacZ* after Cre-mediated excision of a *neo* cassette. Adult R26R/R26CreER^{T2} mice were treated with 175 mg/kg body weight TM for 5 consecutive days, and the recombination of the *lacZ* reporter was analyzed 4 days after the last administration (Fig. 1*A*). Southern analysis of genomic DNA from different organs showed up to 50% recombination (50% in the liver, 30% in the kidney), without detectable background activity in untreated animals, as reported previously (17) (data not shown). Whole-mount tissues from R26R/R26CreER^{T2} mice demonstrated strong β-gal expression in almost all tissues (Fig. 1*A*) except for brain (data not shown). No background recombination was observed in R26R/R26CreER^{T2} mice treated with vehicle (data not shown). The recombination efficiency was also tested during embryogenesis. Female R26R mice mated with male R26CreER^{T2} mice bearing E14.5 embryos were injected i.p. with 200 mg/kg TM. Two days later, tissues from E16.5 embryos were stained with X-gal, demonstrating that

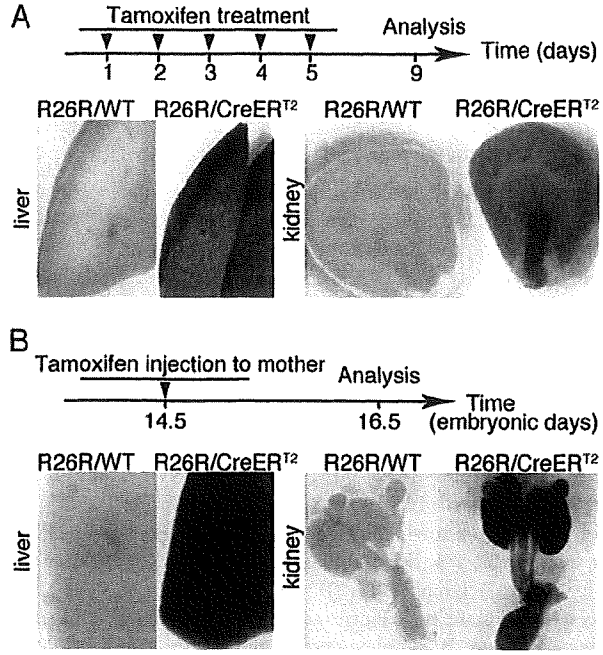

FIGURE 1. TM-inducible LacZ expression in R26R/R26CreER^{T2} mice. *A*, Whole-mount *LacZ* staining of liver and kidney of R26R/R26CreER^{T2} adult mice. R26R/R26CreER^{T2} mice and R26R/WT littermates (R26R/WT) were orally administered 175 mg/kg of TM for 5 consecutive days. Four days later, mice were sacrificed and subjected to X-Gal staining. Only the double transgenic mice exposed to TM showed X-Gal positive staining. *B*, Whole mount *LacZ* staining of tissues in R26R/R26CreER^{T2} embryos. Male R26CreER^{T2} mice were mated with female R26R mice, and pregnant females with E14.5 embryos were injected i.p. with 200 mg/kg TM. Two days later, tissues from E16.5 embryos were stained with X-gal. Only the tissues from double transgenic mice exposed to TM showed X-Gal positive staining.

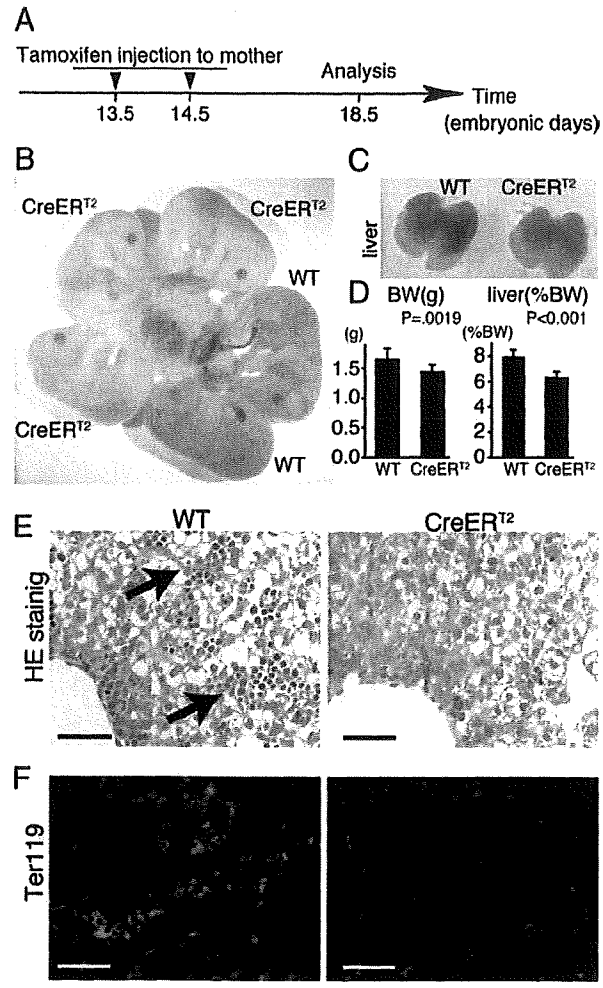

FIGURE 2. Severe anemia in R26CreER^{T2} embryos after the administration of TM. *A*, Pregnant female mice were administered 150 mg/kg TM i.p. at E13.5 and E14.5 and sacrificed at E18.5. *B*, R26CreER^{T2} embryos without floxed alleles were anemic compared with WT embryos. These embryos were treated with TM simultaneously. *C*, The liver of R26CreER^{T2} embryos was anemic and smaller than those of WT littermates. *D*, Body weight and liver weight normalized to body weight were lower in R26CreER^{T2} embryos (n = 5). *E*, Erythroblasts in the embryonic liver (arrow) decreased significantly in R26CreER^{T2} embryos. *F*, Ter119^{+} cells in the embryonic liver decreased in R26Cre-ER^{T2} mice. Bar = 100 μM.

only the tissues from double transgenic mice exposed to TM showed β-gal expression (Fig. 1*B*).

Severe anemia observed in R26CreER^{T2} embryos after the administration of TM

We first noticed the toxicity of R26CreER^{T2} mice when we tried to knockdown the expression of BMP-4 in embryogenesis using R26CreER^{T2} mice, and administered TM to pregnant BMP-4$^{flox/flox}$ mice (33) bearing BMP-4$^{flox/flox}$; R26CreER^{T2} embryos and BMP-4$^{flox/flox}$; WT embryos. In this experiment, 150 mg/kg TM was administered for 2 consecutive days (Fig. 2*A*) to achieve complete recombination in both alleles in BMP-4$^{flox/flox}$ mice. Four days after the last injection, we analyzed the embryos, and observed severe anemia in BMP-4$^{flox/flox}$; R26CreER^{T2} embryos, but not in BMP-4$^{flox/flox}$; Cre^{-} embryos (data not shown). To test whether the phenotype in BMP-4$^{flox/flox}$; R26CreER^{T2} embryos was due to the deletion of BMP-4 gene or due to the systemic activation of CreER^{T2}, we administered the same amount of TM to pregnant WT mice bearing R26CreER^{T2} embryos and WT embryos without a floxed allele. Four days later, R26CreER^{T2} embryos without a floxed allele showed severe anemia as well (Fig. 2*B*), indicating that the anemia was not due to the deletion of floxed alleles, but is due to the toxicity of CreER^{T2}. The livers of R26CreER^{T2} embryos looked pale (Fig. 2*C*), and body weight as well as liver weight of R26CreER^{T2} embryos was lower compared with those of WT embryos (Fig. 2*D*). R26CreER^{T2} embryos treated with vehicle did not show anemia, or the reduction in body weight or liver weight. Histological analysis demonstrated the colonization of erythroblasts in the liver in WT embryos in late embryogenesis, while the number of erythroblast was significantly reduced in R26CreER^{T2} embryos (Fig. 2, *E* and *F*). These hematological changes in R26CreER^{T2} embryos were already evident at E16.5 (supplementary Fig. 1),[4] while the body weight reduction was not observed yet.

Thymus atrophy and hematological abnormality observed in R26CreERT2 adults after the administration of TM

Next, we administered TM to adult R26CreER^{T2} mice and WT littermates according to the protocol shown in Fig. 3*A*. R26CreER^{T2} mice administered TM developed severe thymus atrophy, but not R26CreER^{T2} mice treated with vehicle, nor WT mice treated with TM (Fig. 3*A*). Thymus weight normalized to body weight was significantly reduced in R26CreER^{T2} mice treated with TM (Fig. 3*A*),

[4] The online version of this article contains supplemental material.

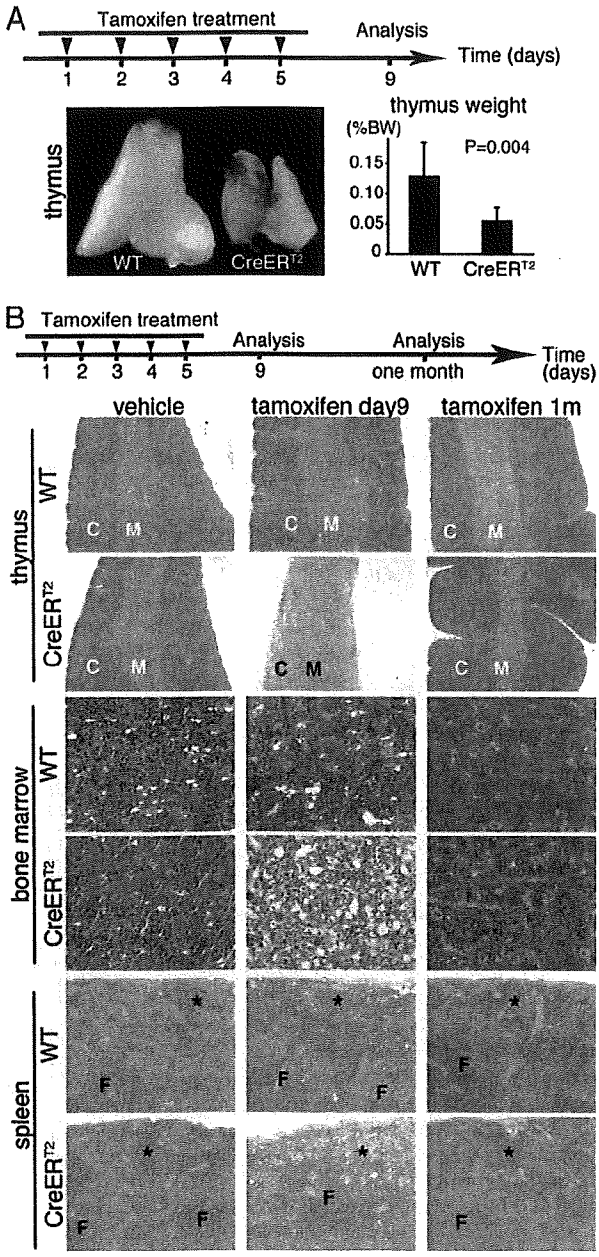

FIGURE 3. Thymus atrophy and hematological abnormality in R26CreER^{T2} adults after the administration of TM. *A*, Eight-week-old R26CreER^{T2} mice and WT littermates were treated with 175 mg/kg of TM orally for 5 consecutive days. Animals were analyzed 4 days after the administration. Representative thymus atrophy and the reduction of thymus weight normalized to body weight in R26CreER^{T2} embryos were shown (n = 5). *B*, Representative histological findings in the thymus, bone marrow, and spleen after 9 days, and 1 mo. R26CreER^{T2} mice exhibited thymus cortical atrophy, hypocellular bone marrow, and decrease of erythroblasts in the red pulp of the spleen at day 9, while these changes were significantly diminished after 1 mo. Cell density in the follicle of the spleen was not changed. C, cortex; M, medulla; F, follicle; *, erythroblasts in red pulp of spleen.

which was consistent with the reduced cell density in the cortical region of the thymus (Fig. 3*B*). R26CreER^{T2} mice treated with TM also exhibited hypocellular bone marrow, and a decrease of erythroblasts in the red pulp of the spleen (Fig. 3*B*, *), but the cell density in the white pulp of the spleen was not changed. We also analyzed whether the strains recover from the hematological abnormality, and demonstrated that the extent of recovery from the hematological toxicity greatly differed among individual mice 2 wk after the administration of TM (supplementary Fig. 2), while all R26CreER^{T2} mice recovered completely after 1 mo (Fig. 3*B*).

CreER^{T2} toxicity affected multiple hematopoietic lineages

We further analyzed the hematopoietic lineages affected by the toxicity. Adult R26CreER^{T2} mice and WT littermates were treated according to the protocol used in Fig. 3, which exerts severe hematological toxicity in R26CreER^{T2} mice. Numbers of cells in the thymus, bone marrow, and spleen decreased in R26CreER^{T2} mice after TM treatment (Fig. 4*A*).

FACS analysis in the thymus demonstrated that CD4$^+$CD8$^+$ double positive cells were significantly reduced in R26CreER^{T2} mice (Fig. 4*B*, DP). In addition, the numbers of the cells in double negative subsets in c-*Kit*/CD25 profiles of Lin$^-$ fraction were reduced in R26CreER^{T2} mice.

We also analyzed Ter119/Mac-1, Gr-1 profile and B220/IgM profile of bone marrow cells (Fig. 4*B*). The numbers of myeloid cells (Mac-1, Gr-1 positive cells), erythroblasts (Ter119$^+$ cells) and immature B lymphocytes (B220$^+$/IgM$^-$ cells) were significantly reduced in the bone marrow of R26CreER^{T2} mice, while the number of mature B lymphocytes did not change (Fig. 4*B*). Together with that the number of CD4$^+$CD8$^+$ double positive cells was significantly reduced in the thymus of R26CreER^{T2} mice, immature cells might be more sensitive to the toxicity of CreER^{T2}.

To analyze the toxicity in the peripheral tissues, we further examined Ter119/Mac-1, Gr-1 profile and B220/IgM profile in the spleen (Fig. 4*B*). Similar to the results in the bone marrow cells, the numbers of myeloid cells and erythroblasts decreased in the spleens of R26CreER^{T2} mice, but not the number of mature B lymphocytes.

Increased apoptosis and attenuated proliferation in the hematopoietic tissues of R26CreER^{T2} mice after the administration of TM

To define the nature of the toxicity of CreER^{T2}, we analyzed apoptosis and cell proliferation in the hematopoietic tissues in adult R26CreER^{T2} mice treated with TM according to the protocol in Fig. 3. These mice were sacrificed at the last day of administration, when viable cells still remain in the hematopoietic tissues (Fig. 5). The numbers of Ki67-positive cells were reduced both in thymus and spleen of R26CreER^{T2} mice, while the numbers of TUNEL-positive cells were increased in spleen, but not in thymus of R26CreER^{T2} mice.

Considering high rate of apoptosis during thymocyte maturation, we postulate that the loss of immature thymocytes in R26CreER^{T2} mice (Fig. 4) might reduce the number of "native" apoptosis, and mask the increased apoptosis due to the toxicity.

Therefore, we conclude that the toxicity of CreER^{T2} is due to attenuated proliferation and increased apoptosis.

Direct toxicity of CreER^{T2} in hematopoietic cells

To exclude the possibility that the hematological abnormality observed in R26CreER^{T2} mice is caused secondarily to unknown systemic disorders, we analyzed the direct effect of TM on hematopoietic cells obtained from R26CreER^{T2} mice. First, we isolated lineage marker negative (Lin$^-$) c-*kit*$^+$ cells from bone marrow and cultured these cells with erythropoietin to induce differentiation into erythroid cells in the presence or absence of 4-hydroxytamoxifen (4-OHT). Ter119$^+$ cells were not generated when 4-OHT was administered to the cells from R26CreER^{T2} mice (Fig. 6*A*). Next, we cultured Lin$^-$c-*kit*$^+$ cells on a monolayer of stromal cell line TSt-4, which efficiently supports the generation of B and myeloid

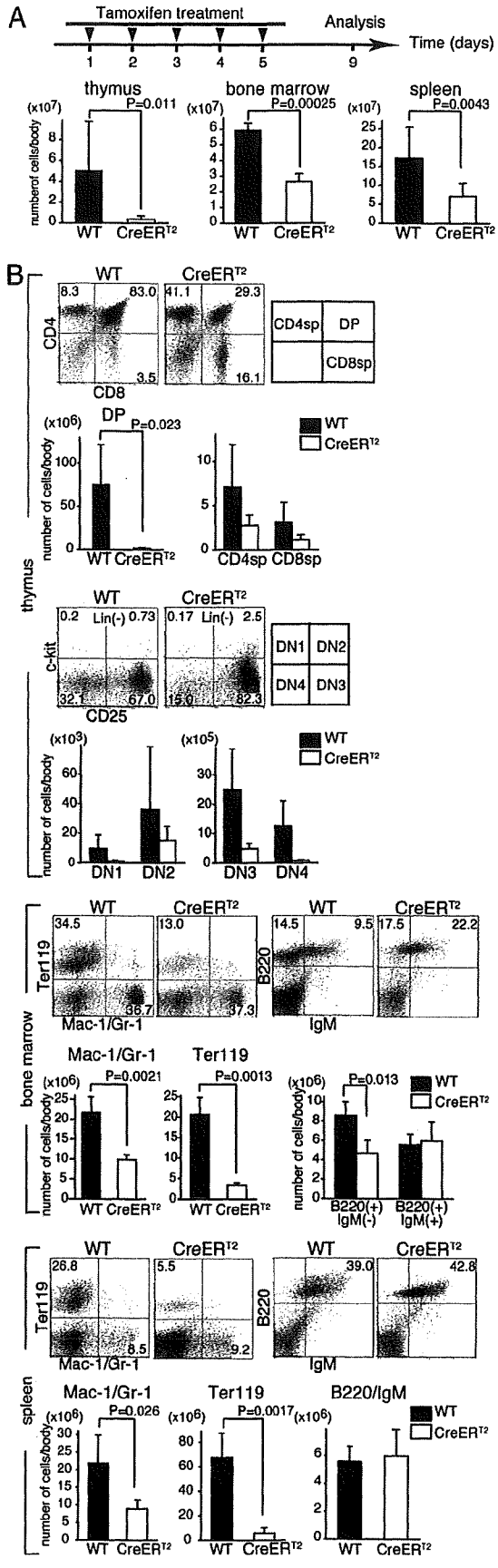

FIGURE 4. FACS analysis of hematopoietic tissues in R26CreER^{T2} mice after the administration of TM. *A*, Mice were treated with 175 mg/kg of TM orally for 5 consecutive days and analyzed at day 9. Total numbers of cells of the thymus (n = 7), bone marrow (n = 3), and spleen (n = 7) decreased in R26CreER^{T2} mice after the administration of TM. *B*, Flow cytometric profiles of hematopoietic cells in the thymus, bone marrow, and spleen after the administration of TM. CD4$^+$CD8$^+$ double positive cells were significantly reduced in the thymus of R26CreER^{T2} mice. In profiles of c-*kit*/CD25, Lin$^-$ fraction was subdivided into c-*kit*$^+$CD25$^-$, c-*kit*$^+$ CD25$^+$, c-*kit*$^-$ CD25$^+$, c-*kit*$^-$ CD25$^-$ subsets, which are designated as DN1, DN2, DN3, and DN4 subsets, respectively. Cell numbers of all subsets were decreased in R26CreER^{T2} mice. The numbers of myeloid cells (Mac-1 or Gr-1 positive cells) and erythroblasts (Ter119$^+$ cells) in the bone marrow and spleen, as well as the number of immature B lymphocytes (B220$^+$/IgM$^-$ cells) in the bone marrow were significantly decreased of R26Cre-ER^{T2} mice (n = 3). The percentages of cells in each quadrant are indicated.

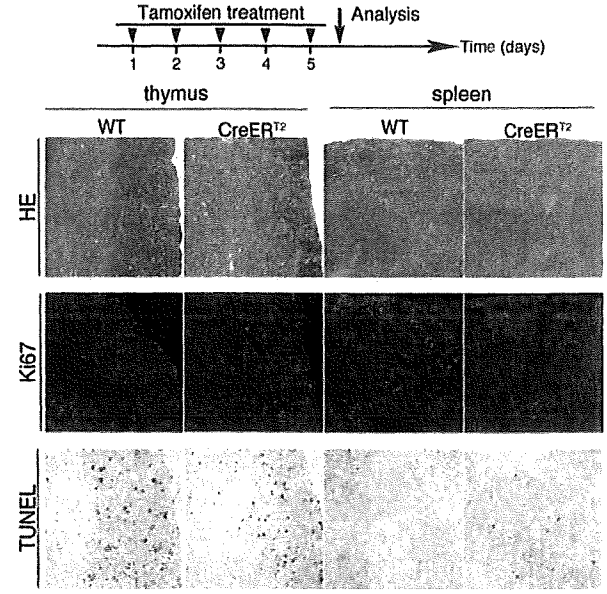

FIGURE 5. Increased apoptosis and attenuated proliferation in the thymus and spleen of R26CreER^{T2} mice after the administration of TM. R26CreER^{T2} mice were treated with 175 mg/kg of TM orally for 5 consecutive days and analyzed at the last day of the administration. The number of Ki67-positive cells was reduced both in the thymus and spleen of R26CreER^{T2} mice, while the number of TUNEL-positive cells was increased in the spleen, but not in the thymus of R26CreER^{T2} mice.

cells, for 14 days, and 4-OHT was administered to the culture at various time points (Fig. 6*B*). The generation of B cells, as examined by the expression of CD19, was significantly reduced by the administration of 4-OHT to the cells from R26CreER^{T2} mice, but not the generation of myeloid cells determined by the expression of Mac-1 (Fig. 6, *B* and *C*). Finally, we analyzed the toxicity of CreER^{T2} in already differentiated hematopoietic cells. We isolated Mac-1$^+$ cells and CD19$^+$ cells from bone marrow and cultured them on a monolayer of TSt-4cells in the presence or absence of 4-OHT. The number of CD19$^+$ cells was significantly reduced when 4-OHT was administered to the cells from R26Cre-ER^{T2} mice, while the number of Mac-1$^+$ cells was not affected (Fig. 6*D*).

Chromosomal abnormalities in bone marrow cells caused by the activation of CreER^{T2}

As the endonuclease activity of Cre is reported to cause chromosomal aberrations and growth arrest in MEF in vitro (18), we analyzed whether the chromosomal aberrations are caused in vivo in hematopoietic cells in R26CreER^{T2} mice. R26CreER^{T2} mice and

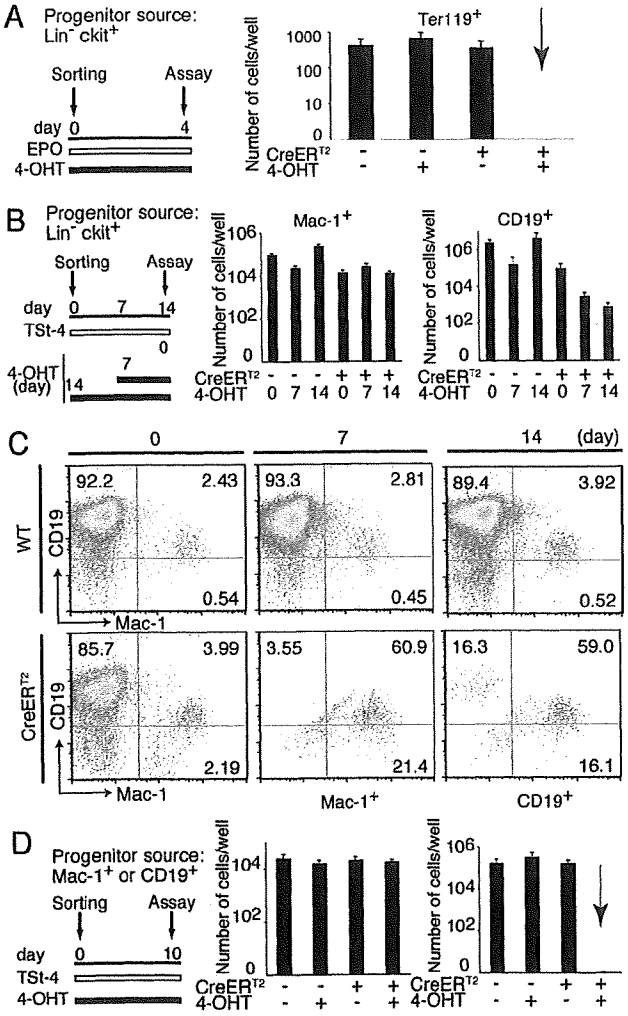

FIGURE 6. In vitro administration of 4-hydroxytamoxifen to the hematopoietic progenitor cells bearing CreER^{T2} arrests proliferation and differentiation. *A*, Lin$^-$c-*kit*$^+$ cells (500 cells) collected from R26CreER^{T2} mice and WT littermates were cultured with erythropoietin (EPO) to induce differentiation into the erythrocyte lineage in the presence or absence of 4-hydroxytamoxifen (4-OHT) at a concentration of 1 μM. Four days later, Ter119$^+$ cells were not generated in the culture where 4-OHT was administered to the cells from R26CreER^{T2} mice. *B*, Lin$^-$c-*kit*$^+$ cells (300 cells) from bone marrow were cultured on a monolayer of stromal cell line TSt-4 for 14 days for myeloid and B lymphoid potentials. 4-OHT added from day 0 (14) or from day 7 (7), and the generation of the B cells examined by the expression of CD19 was significantly reduced in the cells from R26CreER^{T2} mice treated with 4-OHT, but not the generation of myeloid cells determined by the expression of Mac-1. *C*, Representative FACS profiles of the experiment in Fig. 4*B* with their percentages in the respective quadrant. CD19$^+$ cells were eradicated by the administration of 4-OHT to the cells from R26CreER^{T2} mice. *D*, Differentiated Mac-1$^+$ cells and CD19$^+$ cells (10^4 cells for each) were isolated from bone marrow and cultured on a monolayer of TSt-4cells in the presence or absence of 4-OHT. The number of CD19$^+$ cells was significantly reduced when 4-OHT was administered to the cells from R26CreER^{T2} mice, while the number of Mac-1$^+$ cells did not.

WT littermates treated with vehicle or TM for 5 consecutive days were sacrificed 3 days after the last administration (Fig. 7*A*), and bone marrow cells were analyzed for chromosomal numbers and karyotype. In R26CreER^{T2} mice treated with TM only 53% of the cells showed a normal diploid chromosome number of 40 (Fig. 7*B*), while 90% of the cells had 40 chromosomes in WT mouse

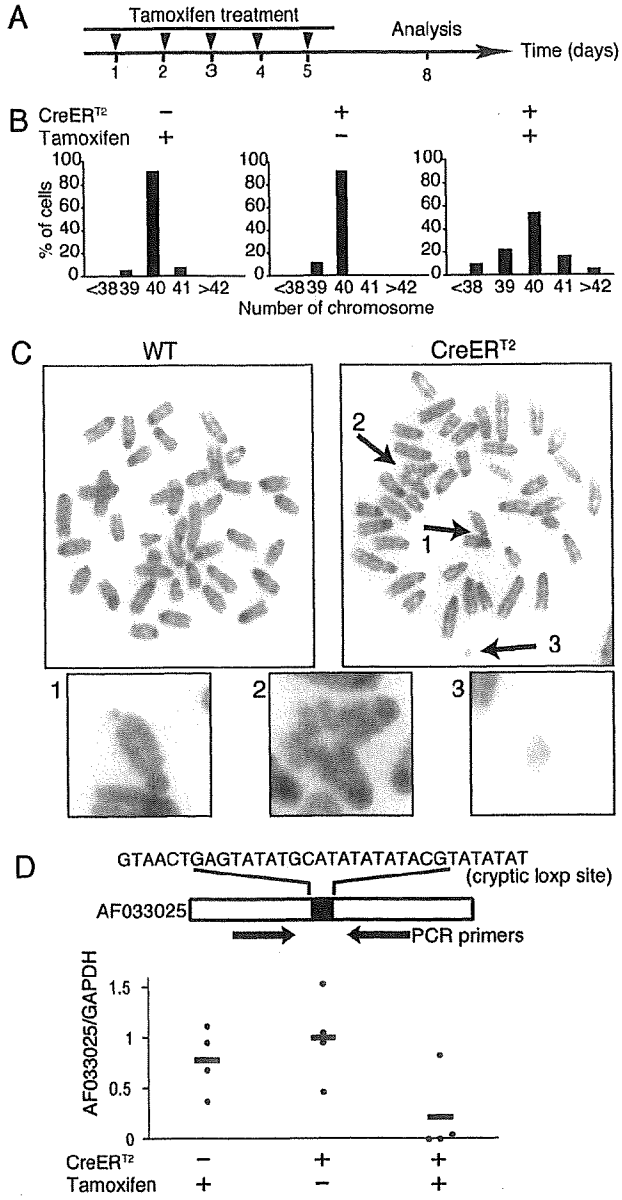

FIGURE 7. Chromosomal abnormalities in bone marrow cells caused by the activation of CreER^{T2}. *A*, Eight-week-old R26CreER^{T2} mice and WT littermates were treated with 175 mg/kg of TM orally for 5 consecutive days, and bone marrow cells were analyzed for chromosomal numbers and karyotype 3 days after the last administration. *B*, In R26CreER^{T2} mice treated with TM (*right*), only 53% of the cells showed a normal diploid chromosome number of 40, while 90% of the cells had 40 chromosomes in WT mouse treated with TM (*left*) as well as in R26CreER^{T2} mouse treated with vehicle (*middle*). *C*, Various types of chromosome abnormalities such as chromosome exchanges (1), chromatic exchanges (2), and chromatid breaks (3) were observed only in R26CreER^{T2} bone marrow cells after the administration of TM in karyotypic analysis. *D*, Cleavage at the cryptic/pseudo *loxP* site in R26CreER^{T2} thymus genome after the administration of TM. We designed real-time PCR primer sets around the reported cryptic/pseudo *loxP* site in AF033025 locus to detect the amount of intact AF033025 locus (5-TGTTGGACGAGGCCACCT-3 and 5-TCCGGCCT TCTCTAGCCTAGA-3). The results were normalized to the amount of GAPDH gene without cryptic/pseudo *loxP* site using the following primers (5-CCAGAACATCATCCCTGCATC-3 and 5-CCTGCTTCACCACCT TCTTGA-3). In three of four R26CreER^{T2} mice, the intact AF033025 locus was almost undetectable after the administration of TM, indicating illegitimate cleavage at the cryptic/pseudo *loxP* site due to the activation of CreER^{T2}.

treated with TM as well as in R26CreER^{T2} mouse treated with vehicle. In karyotype analysis, 78% of bone marrow cells from R26CreER^{T2} mouse treated with TM displayed chromosomal aberrations including chromosome exchanges (Fig. 7*C*, 1), chromatic exchanges (Fig. 7*C*, 2), and chromatid breaks (Fig. 7C, 3), while no chromosomal aberrations were observed in bone marrow cells from WT mice treated with TM (Fig. 7*C*) or in bone marrow cells from R26CreER^{T2} mice treated with vehicle (data not shown).

Thyagarajan et al. (35) reported that mammalian genome contains several candidates for cryptic/pseudo *loxP* sites, and that one locus in mouse genome AF033025 (GenBank) serves as an active site for the Cre recombinase. To clarify whether inappropriate cleavage at cryptic *loxP* sites occurs after the activation of CreER^{T2}, we designed real-time PCR primer sets around the cryptic/pseudo *loxP* site in AF033025 locus to detect the amount of intact AF033025 locus (Fig. 7*D*). Intact AF033025 locus in the thymus of three of four R26CreER^{T2} mice was almost undetectable after the administration of TM, indicating illegitimate cleavage at the cryptic/pseudo *loxP* site due to the activation of CreER^{T2}. The amount of intact AF033025 locus did not change until the administration of TM, excluding the possibility that the gene targeting procedure to generate R26CreER^{T2} allele altered the locus.

Discussion

In this study, we demonstrated that the administration of TM to R26CreER^{T2} mice causes severe growth arrest, apoptosis, and illegitimate chromosomal rearrangement in hematopoietic cells, even in the absence of genes targeted by *loxP* sites. We tested two independent lines of R26CreER^{T2} mice from different facilities, and the results were essentially the same. Furthermore, both strains recovered from the toxicity within a month. We also performed in vitro culturing of hematopoietic cells from these mice and demonstrated direct toxicity of CreER^{T2} on growth and differentiation of certain cell types.

Hematological abnormalities in R26CreER^{T2} mice is due to systemic activation of CreER^{T2}

Previous reports regarding the adverse effects of Cre in vivo could not exclude the possibility that the unexpected phenotypes were due to the disruption of the genome loci where transgenes were integrated. On the contrary, the lines in this report are alleles introduced into the well-characterized R26 locus, and the disruption of the locus was proved not to cause adverse effects. In addition, no hematological abnormalities were detected until the administration of TM, indicating that an effect of the R26 locus is not likely to be the cause. Importantly, the hematological abnormalities was not due to the toxicity of TM, because the administration of TM to WT mice in vivo as well as to the hematopoietic cells from WT mice in vitro did not exert any effect. Therefore, we concluded that the hematological abnormalities observed in this report were due to the systemic activation of CreER^{T2}, which arrested cell proliferation and induced apoptosis (Fig. 5), and were the direct effect on hematopoietic cells (Fig. 6).

The cause of these hematological abnormalities after the systemic activation of CreER^{T2} is likely to be Cre-mediated genomic rearrangements as observed in Fig. 7, perhaps at cryptic or pseudo-*loxP* sites within the mouse genome, which have recently been shown to serve as substrates for Cre recombinase (34, 35). Thygarajan et al. (35) reported that the sequences in mouse genomes considerably divergent from the consensus *loxP* sites serve as functional recognition sites for Cre mediated recombination, and the recombination efficiency of one locus (AF033025) was considerably high in bacterial assays. We further demonstrated that intact AF033025 locus in three of four R26CreER^{T2} mice was almost undetectable after the administration of TM (Fig. 7*D*). Furthermore, recent bioinformatics analysis estimated the frequency of cryptic *loxP* sites in the mouse genome is 1.2 per megabase, and are homogeneously distributed throughout the genome.

High sensitivity of hematopoietic cells to the systemic activation of CreER^{T2} might be due to their rapid proliferation rate, because the genome in rapidly proliferating cells are more easily accessible by CreER^{T2} than the tightly packed genome in quiescent cells. FACS analysis also demonstrated that immature proliferating cells in each hematopoietic lineage tend be more sensitive to CreER^{T2} toxicity (Fig. 4*B*). Positive correlation between Cre-induced toxicity and proliferation was previously reported in fibroblasts (18) as well as in transgenic flies (36). In addition to hematopoietic cells, intestinal epithelial cells also proliferate rapidly, and R26CreER^{T2} mice occasionally demonstrated diarrhea and intestinal edema after the administration of TM, possibly due to the toxicity of CreER^{T2} in rapidly proliferating intestinal epithelial cells (data not shown).

Sensitivity to the toxicity of CreER^{T2} might also be influenced by the amount of CreER^{T2} translocating to nuclei, which is defined by the level of CreER^{T2} expression as well as dose and tissue distribution of TM. Seibler et al. (17) previously reported relatively high expression of CreER^{T2} in thymus, where we observed severe toxicity.

Which is tolerated better, CreER^{T2} or Cre?

In previous reports demonstrating adverse effects in Cre transgenic mice, the authors suggested that the inducible form of Cre might be tolerated better because it stays outside the nucleus until induction (23). However, our results in this study indicated large amount of activated CreER^{T2} was also able to cause cell toxicity. Although the growth arrest is prominent in CD19^{+} cells from R26CreER^{T2} mice after the administration of TM (Fig. 6), no hematological abnormalities have been reported in well-characterized CD19-Cre mice, in which Cre recombinase is highly expressed in B cells. One explanation for the discrepancy is that DNA damage in the cells bearing Cre recombinase induces the cells to develop DNA repairing system to counteract the damage, and such systems might be established in CD19-Cre mice, while R26CreER^{T2} mice are not prepared when massive amounts of CreER^{T2} would be suddenly activated and cause DNA damage.

To make good use of R26CreERT2 mice, which are still attractive

Although the hematological abnormality in R26CreER^{T2} mice might compromise the phenotypic analysis of the gene of interest, the strain is still of great value because of its efficient inducibility without leakage, and of ubiquitous expression of CreER^{T2}.

In this study, we suggest three points to take note of to make good use of this strain. One way to solve the problem is taking appropriate control for Cre toxicity: the use of the same mouse without floxed allele. In spite of the fact that Cre toxicity has been occasionally documented in the literatures, it seems still to be widely neglected. A recent study has systemically reviewed the use of RIP-Cre mice, which alone display glucose intolerance, and demonstrated that in more than half of the cases, the appropriate control was not included (23).

Second, it is better to postpone the analysis of the mice for at least 1 mo after the administration of TM. The hematological abnormalities will have diminished after 1 mo (Fig. 3*B*), possibly due to the proliferation of the surviving cells.

Third, it is better to minimize the dose of TM. The toxicity in R26CreER^{T2} mice was dependent on the dose of TM, which regulates the inducibility of CreER^{T2}. The minimal dose of TM to

induce efficient recombination varies between target alleles, depending on the number of floxed alleles, the distance between *loxP* sites, the expression level of the target gene, and local chromatin structure. One should adjust the minimal dose of TM to induce efficient recombination in the gene of the interest (supplementary Fig. 3). In cell culture analysis, changing the medium after incubation for 6 h with 4-OHT minimizes the toxicity with efficient recombination (data not shown). The experiments where high recombination efficiency is not necessary or even desirable, such as lineage tracing and mosaic oncogene activation, might be ideal for R26CreER^{T2} mice. The self-excising Cre vectors might be another option to reduce the toxicity (37–39).

Therapeutic implications and possibility to be a disease model

The result of the study warns of the potential consequences of Cre-mediated recombination between cryptic *loxP* sites in the genome in Cre/*loxP* based technologies in human gene therapy protocols. Paradoxically, however, immature and rapidly proliferating cells are more susceptible to the toxicity caused by the activation of CreER^{T2}, indicating the possible therapeutic implication of the technology for cancer treatment. Schimidt-Supprian et al. (40) reported that the activation of CreER^{T2} transgene in c-Myc-driven primary B cell lymphoma leads to death of lymphoma at lower dose of TM compared with our experiment. Because the dose of TM they used in their experiment does not exert severe toxicity in healthy hematopoietic cells (data not shown), selective eradication of malignant cells might be possible. In addition, R26CreER^{T2} mice might be useful as an inducible model for hematological abnormalities caused by aberrant chromosomal rearrangements.

Acknowledgments

We thank Drs. Y. Kaziro, Y. Nabeshima, S. Takeda, and T. Sakurai for valuable comments and discussion. We also appreciate Drs. D. Sakata, T. Matsuoka, N. Watanabe, and S. Narumiya for providing the experimental equipment.

Disclosures

The authors have no financial conflict of interest.

References

1. Lewandoski, M. 2001. Conditional control of gene expression in the mouse. *Nat. Rev.* 2: 743–755.
2. Mansuy, I. M., and U. Suter. 2000. Mouse genetics in cell biology. *Exp. Physiol.* 85: 661–679.
3. Nagy, A. 2000. Cre recombinase: the universal reagent for genome tailoring. *Genesis* 26: 99–109.
4. Sternberg, N., and D. Hamilton. 1981. Bacteriophage P1 site-specific recombination, I: recombination between loxP sites. *J. Mol. Biol.* 150: 467–486.
5. Sternberg, N., D. Hamilton, S. Austin, M. Yarmolinsky, and R. Hoess. 1981. Site-specific recombination and its role in the life cycle of bacteriophage P1. *Cold Spring Harbor Symp. Quant. Biol.* 45 Pt. 1: 297–309.
6. Branda, C. S., and S. M. Dymecki. 2004. Talking about a revolution: The impact of site-specific recombinases on genetic analyses in mice. *Development. Cell* 6: 7–28.
7. Metzger, D., and R. Feil. 1999. Engineering the mouse genome by site-specific recombination. *Curr. Opin. Biotechnol.* 10: 470–476.
8. Rajewsky, K., H. Gu, R. Kuhn, U. A. Betz, W. Muller, J. Roes, and F. Schwenk. 1996. Conditional gene targeting. *J. Clin. Invest.* 98: 600–603.
9. Utomo, A. R., A. Y. Nikitin, and W. H. Lee. 1999. Temporal, spatial, and cell type-specific control of Cre-mediated DNA recombination in transgenic mice. *Nat. Biotechnol.* 17: 1091–1096.
10. Kuhn, R., F. Schwenk, M. Aguet, and K. Rajewsky. 1995. Inducible gene targeting in mice. *Science* 269: 1427–1429.
11. Feil, R., J. Brocard, B. Mascrez, M. LeMeur, D. Metzger, and P. Chambon. 1996. Ligand-activated site-specific recombination in mice. *Proc. Natl. Acad. Sci. USA* 93: 10887–10890.
12. Brocard, J., X. Warot, O. Wendling, N. Messaddeq, J. L. Vonesch, P. Chambon, and D. Metzger. 1997. Spatio-temporally controlled site-specific somatic mutagenesis in the mouse. *Proc. Natl. Acad. Sci. USA* 94: 14559–14563.
13. Danielian, P. S., D. Muccino, D. H. Rowitch, S. K. Michael, and A. P. McMahon. 1998. Modification of gene activity in mouse embryos in utero by a tamoxifen-inducible form of Cre recombinase. *Curr. Biol.* 8: 1323–1326.
14. Leone, D. P., S. Genoud, S. Atanasoski, R. Grausenburger, P. Berger, D. Metzger, W. B. Macklin, P. Chambon, and U. Suter. 2003. Tamoxifen-inducible glia-specific Cre mice for somatic mutagenesis in oligodendrocytes and Schwann cells. *Mol. Cell. Neurosci.* 22: 430–440.
15. Vooijs, M., J. Jonkers, and A. Berns. 2001. A highly efficient ligand-regulated Cre recombinase mouse line shows that LoxP recombination is position dependent. *EMBO Reports* 2: 292–297.
16. Lantinga-van Leeuwen, I. S., W. N. Leonhard, A. van de Wal, M. H. Breuning, S. Verbeek, E. de Heer, and D. J. Peters. 2006. Transgenic mice expressing tamoxifen-inducible Cre for somatic gene modification in renal epithelial cells. *Genesis* 44: 225–232.
17. Seibler, J., B. Zevnik, B. Kuter-Luks, S. Andreas, H. Kern, T. Hennek, A. Rode, C. Heimann, N. Faust, G. Kauselmann, et al. 2003. Rapid generation of inducible mouse mutants. *Nucleic Acids Res.* 31: e12.
18. Loonstra, A., M. Vooijs, H. B. Beverloo, B. A. Allak, E. van Drunen, R. Kanaar, A. Berns, and J. Jonkers. 2001. Growth inhibition and DNA damage induced by Cre recombinase in mammalian cells. *Proc. Natl. Acad. Sci. USA* 98: 9209–9214.
19. Silver, D. P., and D. M. Livingston. 2001. Self-excising retroviral vectors encoding the Cre recombinase overcome Cre-mediated cellular toxicity. *Mol. Cell* 8: 233–243.
20. de Alboran, I. M., R. C. O'Hagan, F. Gartner, B. Malynn, L. Davidson, R. Rickert, K. Rajewsky, R. A. DePinho, and F. W. Alt. 2001. Analysis of c-myc function in normal cells via conditional gene-targeted mutation. *Immunity* 14: 45–55.
21. Schmidt, E. E., D. S. Taylor, J. R. Prigge, S. Barnett, and M. R. Capecchi. 2000. Illegitimate Cre-dependent chromosome rearrangements in transgenic mouse spermatids. *Proc. Natl. Acad. Sci. USA* 97: 13702–13707.
22. Buerger, A., O. Rozhitskaya, M. C. Sherwood, A. L. Dorfman, E. Bisping, E. D. Abel, W. T. Pu, S. Izumo, and P. Y. Jay. 2006. Dilated cardiomyopathy resulting from high-level myocardial expression of Cre-recombinase. *J. Card. Fail.* 12: 392–398.
23. Lee, J. Y., M. Ristow, X. Lin, M. F. White, M. A. Magnuson, and L. Hennighausen. 2006. RIP-Cre revisited, evidence for impairments of pancreatic β-cell function. *J. Biol. Chem.* 281: 2649–2653.
24. Naiche, L. A., and V. E. Papaioannou. 2007. Cre activity causes widespread apoptosis and lethal anemia during embryonic development. *Genesis* 45: 768–775.
25. Valenzuela, D. M., A. J. Murphy, D. Frendewey, N. W. Gale, A. N. Economides, W. Auerbach, W. T. Poueymirou, N. C. Adams, J. Rojas, J. Yasenchak, et al. 2003. High-throughput engineering of the mouse genome coupled with high-resolution expression analysis. *Nat. Biotechnol.* 21: 652–659.
26. Soriano, P. 1999. Generalized lacZ expression with the ROSA26 Cre reporter strain. *Nat. Genet.* 21: 70–71.
27. Tanaka, M., S. Endo, T. Okuda, A. N. Economides, D. M. Valenzuela, A. J. Murphy, E. Robertson, T. Sakurai, A. Fukatsu, G. D. Yancopoulos, T. Kita, and M. Yanagita. 2008. Expression of BMP-7 and USAG-1 (a BMP antagonist) in kidney development and injury. *Kidney Int.* 73: 181–191.
28. Yanagita, M. 2006. Modulator of bone morphogenetic protein activity in the progression of kidney diseases. *Kidney Int.* 70: 989–993.
29. Yanagita, M., Y. Ishimoto, H. Arai, K. Nagai, T. Ito, T. Nakano, D. J. Salant, A. Fukatsu, T. Doi, and T. Kita. 2002. Essential role of Gas6 for glomerular injury in nephrotoxic nephritis. *J. Clin. Invest.* 110: 239–246.
30. Yanagita, M., T. Okuda, S. Endo, M. Tanaka, K. Takahashi, F. Sugiyama, S. Kunita, S. Takahashi, A. Fukatsu, M. Yanagisawa, et al. 2006. Uterine sensitization-associated gene-1 (USAG-1), a novel BMP antagonist expressed in the kidney, accelerates tubular injury. *J. Clin. Invest.* 116: 70–79.
31. Masuda, K., H. Kubagawa, T. Ikawa, C. C. Chen, K. Kakugawa, M. Hattori, R. Kageyama, M. D. Cooper, N. Minato, Y. Katsura, and H. Kawamoto. 2005. Prethymic T-cell development defined by the expression of paired immunoglobulin-like receptors. *EMBO J.* 24: 4052–4060.
32. Sugawara, A., K. Goto, Y. Sotomaru, T. Sofuni, and T. Ito. 2006. Current status of chromosomal abnormalities in mouse embryonic stem cell lines used in Japan. *Comp. Med.* 56: 31–34.
33. Jiao, K., H. Kulessa, K. Tompkins, Y. Zhou, L. Batts, H. S. Baldwin, and B. L. Hogan. 2003. An essential role of Bmp4 in the atrioventricular septation of the mouse heart. *Genes Dev.* 17: 2362–2367.
34. Semprini, S., T. J. Troup, N. Kotelevtseva, K. King, J. R. Davis, L. J. Mullins, K. E. Chapman, D. R. Dunbar, and J. J. Mullins. 2007. Cryptic loxP sites in mammalian genomes: genome-wide distribution and relevance for the efficiency of BAC/PAC recombineering techniques. *Nucleic Acids Res.* 35: 1402–1410.
35. Thyagarajan, B., M. J. Guimaraes, A. C. Groth, and M. P. Calos. 2000. Mammalian genomes contain active recombinase recognition sites. *Gene* 244: 47–54.
36. Heidmann, D., and C. F. Lehner. 2001. Reduction of Cre recombinase toxicity in proliferating *Drosophila* cells by estrogen-dependent activity regulation. *Dev. Genes Evol.* 211: 458–465.
37. Bunting, M., K. E. Bernstein, J. M. Greer, M. R. Capecchi, and K. R. Thomas. 1999. Targeting genes for self-excision in the germ line. *Genes Dev.* 13: 1524–1528.
38. Mahonen, A. J., K. J. Airenne, M. M. Lind, H. P. Lesch, and S. Yla-Herttuala. 2004. Optimized self-excising Cre-expression cassette for mammalian cells. *Biochem. Biophys. Res. Commun.* 320: 366–371.
39. Pfeifer, A., E. P. Brandon, N. Kootstra, F. H. Gage, and I. M. Verma. 2001. Delivery of the Cre recombinase by a self-deleting lentiviral vector: efficient gene targeting in vivo. *Proc. Natl. Acad. Sci. USA* 98: 11450–11455.
40. Schmidt-Supprian, M., and K. Rajewsky. 2007. Vagaries of conditional gene targeting. *Nat. Immunol.* 8: 665–668.

Journal of Cellular Physiology

Orderly Hematopoietic Development of Induced Pluripotent Stem Cells via Flk-1$^+$ Hemoangiogenic Progenitors

AKIRA NIWA,[1,2] KATSUTSUGU UMEDA,[1] HSI CHANG,[1] MEGUMU SAITO,[1,2] KEISUKE OKITA,[3] KAZUTOSHI TAKAHASHI,[3] MASATO NAKAGAWA,[3,4] SHINYA YAMANAKA,[3,4] TATSUTOSHI NAKAHATA,[1,2] AND TOSHIO HEIKE[1]*

[1]*Department of Pediatrics, Graduate School of Medicine, Kyoto University, Kyoto, Japan*

[2]*Clinical Application Department, Center for iPS cell Research and Application (CiRA), Institute for Integrated Cell-Material Sciences, Kyoto University, Kyoto, Japan*

[3]*Basic Biology Department, Center for iPS cell Research and Application (CiRA), Institute for Integrated Cell-Material Sciences, Kyoto University, Kyoto, Japan*

[4]*Department of Stem Cell Biology, Institute for Frontier Medical Sciences, Kyoto University, Kyoto, Japan*

Induced pluripotent stem (iPS) cells, reprogrammed somatic cells with embryonic stem (ES) cell-like characteristics, are generated by the introduction of combinations of specific transcription factors. Little is known about the differentiation of iPS cells in vitro. Here we demonstrate that murine iPS cells produce various hematopoietic cell lineages when incubated on a layer of OP9 stromal cells. During this differentiation, iPS cells went through an intermediate stage consisting of progenitor cells that were positive for the early mesodermal marker Flk-1 and for the sequential expression of other genes that are associated with hematopoietic and endothelial development. Flk-1$^+$ cells differentiated into primitive and definitive hematopoietic cells, as well as into endothelial cells. Furthermore, Flk-1$^+$ populations contained common bilineage progenitors that could generate both hematopoietic and endothelial lineages from single cells. Our results demonstrate that iPS cell-derived cells, like ES cells, can follow a similar hematopoietic route to that seen in normal embryogenesis. This finding highlights the potential use of iPS cells in clinical areas such as regenerative medicine, disease investigation, and drug screening.
J. Cell. Physiol. 221: 367–377, 2009.

Because of their pluripotency and potential for self-renewal, embryonic stem (ES) cells have been used in various fields of science, including developmental biology (Evans and Kaufman, 1981). ES cells can differentiate into multiple cell types in a similar way to that observed in vivo. Previous studies using normal or gene-manipulated ES cells have helped to elucidate the process of normal embryogenesis and the genetic mechanisms of some diseases (Lensch and Daley, 2006).

Hematopoietic and endothelial development are regarded as particularly good processes for comparing the potential of ES cells cultivated in vitro with those grown in vivo (Nakano et al., 1994, 1996; Nishikawa et al., 1998). During embryogenesis, the developmental progression to a hematopoietic lineage is closely associated with progression to an endothelial lineage (Shalaby et al., 1997; Wood et al., 1997; Choi et al., 1998; Garcia-Porrero et al., 1998). Both cell lineages emerge from common mesodermal progenitors called hemangioblasts, which are positive for the vascular endothelial growth factor receptor Flk-1 (Flamme et al., 1995; Risau, 1995; Risau and Flamme, 1995; Choi et al., 1998; Huber et al., 2004). Thereafter, the site of hematopoiesis shifts from the yolk sac (primitive hematopoiesis) to the fetal liver, the spleen, and finally to the bone marrow (definitive hematopoiesis), and is accompanied by a change in the type of hemoglobin produced by erythrocytes (Moore and Metcalf, 1970; Matsuoka et al., 2001). Orderly hematopoietic development can be induced from murine and primate ES cells by various culture methods (Doetschman et al., 1985; Leder et al., 1985, 1992; Nakano et al., 1994, 1996; Xu et al., 2001; Umeda et al., 2004, 2006; Shinoda et al., 2007).

ES cells have been proposed as a potential new source of transplantable cells in regenerative medicine. It is anticipated that in the future such ES-derived cells may be used as sources of hematopoietic cells for stem cell transplants, or of mature blood cells for transfusion therapies. Recent studies have already shown that hematopoietic cells derived from murine ES cells overexpressing HoxB4 or Stat5 can replenish the bone marrow of lethally irradiated recipient mice (Kyba et al., 2002, 2003). However, there are various impediments to the clinical application of ES cells. For example, because they are established from the inner-cell masses of blastocysts, ES cells are subject to the controversy surrounding the manipulation of oocytes. Furthermore, the therapeutic use of ES cells from other individuals carries the risk of immunological complications.

Murine and human induced pluripotent stem (iPS) cells have recently been established from somatic cells by retrovirally introducing certain combinations of genes, such as octamer 3/4

The authors indicate no potential conflicts of interest.

Contract grant sponsor: Ministry of Education, Culture, Sports, Science, and Technology of Japan.

*Correspondence to: Toshio Heike, Department of Pediatrics, Graduate School of Medicine, Kyoto University, 54 Kawahara-cho, Shogoin, Sakyo-ku, Kyoto 606-8507, Japan.
E-mail: heike@kuhp.kyoto-u.ac.jp

Received 20 March 2009; Accepted 19 May 2009

Published online in Wiley InterScience (www.interscience.wiley.com.), 26 June 2009.
DOI: 10.1002/jcp.21864